

AD-783 904

**ELECTROMAGNETIC NOISE INDUCED BY OCEAN
WAVES: I. ELECTROMAGNETIC FIELD IN-
DUCED BY PROGRESSIVE OCEAN WAVES**

Walter Podney

Physical Dynamics, Incorporated

Prepared for:

**Rome Air Development Center
Advanced Research Projects Agency**

March 1974

DISTRIBUTED BY:

NTIS

**National Technical Information Service
U. S. DEPARTMENT OF COMMERCE
5285 Port Royal Road, Springfield Va. 22151**

UNCLASSIFIED

SECURITY CLASSIFICATION OF THIS PAGE (When Data Entered)

REPORT DOCUMENTATION PAGE		READ INSTRUCTIONS BEFORE COMPLETING FORM
1. REPORT NUMBER RADC-TR-74-131	2. GOVT ACCESSION NO.	3. RECIPIENT'S CATALOG NUMBER AD 783 904
4. TITLE (and Subtitle) Electromagnetic Noise Induced by Ocean Waves: I. Electromagnetic Field Induced by Progressive Ocean Waves		5. TYPE OF REPORT & PERIOD COVERED Semi-Annual Tech. Rpt.
		6. PERFORMING ORG. REPORT NUMBER PD-74-060
7. AUTHOR(s) Walter Podney		8. CONTRACT OR GRANT NUMBER(s) F30602-72-C-0495
9. PERFORMING ORGANIZATION NAME AND ADDRESS Physical Dynamics, Inc. PO Box 24 McLean, VA 22101		10. PROGRAM ELEMENT, PROJECT, TASK AREA & WORK UNIT NUMBERS 62301D 21240201
11. CONTROLLING OFFICE NAME AND ADDRESS Defense Advanced Research Projects Agency 1400 Wilson Blvd Arlington, VA 22209		12. REPORT DATE March 74
14. MONITORING AGENCY NAME & ADDRESS (if different from Controlling Office) RADC/OCSE ATTN: L. Strauss Griffiss AFB NY 13441		13. NUMBER OF PAGES 104
		15. SECURITY CLASS. (of this report) UNCLASSIFIED
		15a. DECLASSIFICATION/DOWNGRADING SCHEDULE
16. DISTRIBUTION STATEMENT (of this Report) Approved for public release. Distribution unlimited.		
17. DISTRIBUTION STATEMENT (of the abstract entered in Block 20, if different from Report) Approved for public release. Distribution unlimited.		
18. SUPPLEMENTARY NOTES		
19. KEY WORDS (Continue on reverse side if necessary and identify by block number) Electromagnetic fields Boundary value problems Ocean waves Ampere's law Faraday's law		
20. ABSTRACT (Continue on reverse side if necessary and identify by block number) A general solution is developed for the electromagnetic field induced by an irrotational flow field using Ampere's and Faraday's laws. It is shown that the field is determined by an electromagnetic potential function and a velocity potential function. Solutions corresponding to progressive surface and internal waves for deep and shallow seas are then developed. They are discussed in terms of the fields produced in both polar and equatorial regions.		

ELECTROMAGNETIC NOISE INDUCED BY OCEAN WAVES:
I. ELECTROMAGNETIC FIELD INDUCED BY
PROGRESSIVE OCEAN WAVES

Walter Podney

Contractor: Physical Dynamics, Incorporated
Contract Number: F30602-72-C-0495
Effective Date of Contract: 1 March 1972
Contract Expiration Date: 31 July 1974
Amount of Contract: \$124,914.00
Program Code Number: 4E20

Principal Investigator: Dr. Walter Podney
Phone: 703 790-1188

Project Engineer: Leonard Strauss
Phone: 315 330-3055

Approved for public release;
distribution unlimited.

This research was supported by the
Defense Advanced Research Projects
Agency of the Department of Defense
and was monitored by Leonard Strauss
RADC (OCSE), GAFB, NY 13441 under
Contract F30602-72-C-0495.

12

PUBLICATION REVIEW

This technical report has been reviewed and is approved.

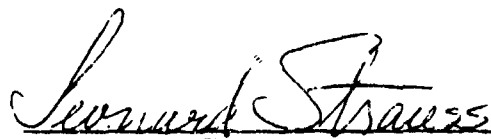

RADC Project Engineer

TABLE OF CONTENTS

	<u>Page</u>
SUMMARY	v
I. INTRODUCTION	1
II. ELECTROMAGNETIC FIELDS INDUCED BY OCEAN WAVES	5
A. PARTICULAR SOLUTION	7
B. HOMOGENEOUS SOLUTION.....	7
C. GENERAL SOLUTION	9
D. PROGRESSIVE WAVE SOLUTION.....	10
III. ELECTROMAGNETIC FIELDS INDUCED BY PROGRESSIVE WAVES IN A DEEP OCEAN	17
A. SURFACE WAVES	17
B. INTERNAL WAVES	28
IV. ELECTROMAGNETIC FIELDS INDUCED BY PROGRESSIVE WAVES IN SHALLOW SEAS	41
A. SURFACE WAVES	41
B. INTERNAL WAVES	47
V. CONCLUSION	55
FIGURE CAPTIONS	60
REFERENCES	89
APPENDIX. PROFILES OF ELECTROMAGNETIC POTENTIALS	91
A. ELECTROMAGNETIC POTENTIAL PROFILE GENERATED BY SURFACE WAVES	91
B. ELECTROMAGNETIC POTENTIAL PROFILE GENERATED BY INTERNAL WAVES	94

SUMMARY

Sea water oscillating across the Earth's magnetic field induces eddy currents in the sea that generate an electromagnetic field characteristic of the velocity field in the sea. The electromagnetic field is the sum of an electrostatic type field, resulting from accumulation of surface charge, and a transverse electric type field having an impedance proportional to phase speeds of ocean waves, which are no greater than a few hundred meters/sec for surface waves and of the order of 1 m/sec or less for internal waves. The electrostatic part of the field vanishes in polar regions and is strongest in equatorial regions. Conversely, the transverse electric part of the field is strongest in polar regions and weakest in equatorial regions.

Magnitude of the electrostatic part of the field produced by a one meter high surface wave progressing across magnetic meridians in equatorial regions increases with wave frequency for wavelengths less than an ocean depth and reaches a lower limiting value of the order of a few microvolts/m² at wavelengths greater than an ocean depth. Above the surface, the electric field vector is circularly polarized in a vertical plane containing the direction of wave propagation and rotates in an opposite sense to the velocity vector of the wave. Immediately below the surface, polarization is elliptical with the same sense of rotation as the velocity vector. At the ocean floor, the field is linearly polarized in a vertical direction, so that the electrostatic part of the field vanishes below the ocean floor.

Similarly, the electrostatic part of the field produced by an internal wave vanishes both above and below the ocean, as the surface displacement resulting from an internal wave is negligible. Polarization of the field within the sea is elliptical with the same sense of rotation as the velocity vector of an internal wave. Magnitude of the field per unit wave height at a thermocline increases with frequency for wavelengths less than a thermocline depth and reaches a lower limiting value of the order of a few tenths of microvolts/m² at wavelengths greater than a thermocline depth.

Surface magnitudes of both the electric and magnetic components of the transverse electric part of the field decrease with wave number for wavelengths of surface and/or internal waves less than an ocean depth. Field strengths per unit wave height produced by surface waves in polar regions attain maximum values of the order of a few microvolts/m² and a few tens of gamma/m for wavelengths much greater than an ocean depth. Internal waves produce maximum field strengths at the surface in polar regions of the order of 10⁻⁴ microvolts/m² and 0.1 gamma/m at wavelengths of the order of an ocean depth. In equatorial regions, maximum field strengths are less than polar values by about a factor of two, for waves progressing along magnetic meridians. The transverse electric part of the field vanishes for waves propagating across magnetic meridians in equatorial regions.

The magnetic vector of the transverse electric part of the field is polarized in a vertical plane containing the direction of wave propagation, and the electric field, by definition, is linearly polarized in a horizontal direction transverse to the direction of wave propagation. Polarization of the magnetic field below the surface exhibits a complicated pattern with both depth and latitude. At and above the surface, however, the magnetic field is always circularly polarized with a sense of rotation opposite to that of the velocity field.

I. INTRODUCTION

As Faraday [1832] first recognized, sea water moving across the Earth's magnetic field induces an electric current in a sea. First investigations of the effect were concerned with measurement of electric fields induced by steady ocean currents. Efforts culminated in development of a so-called geomagnetic electrokinetographic or GEK method [von Arx, 1950] of inferring velocities of broad, steady ocean currents from measurements* of horizontal gradients in the electric potential at the ocean surface. Longuet-Higgins, et al. [1954] develop a sound basis for interpreting GEK measurements.

Although Longuet-Higgins, et al. [1954] consider electric fields and currents produced by ocean waves as well as steady currents, investigation of magnetic effects of either steady currents or ocean waves has been largely neglected until recently. Crews and Futterman [1962] are among the first to investigate magnetic fields produced by ocean waves. They neglect magnetic induction effects, however, and, by using the integral form of Ampere's law, determine magnetic fields produced above the ocean surface by slowly varying currents in a deep ocean. Varburton and Caminiti [1964] extend the analysis to determine magnetic fields produced below the surface of a deep ocean, and Groskaya, et al. [1972], to shallow seas.

* Potential gradients are measured by towing electrodes separated by distances of a few tens of meters behind a ship.

A quasistatic approximation (neglecting magnetically induced electric fields) is perhaps most appropriate for determining magnetic fields induced by tidal motions where vorticity produced by Coriolis forces is important. For motions having periods appreciably less than tidal periods, however, flow fields are effectively irrotational, and magnetic induction effects are readily included.

Weaver [1965] is the first to have accounted for magnetic induction effects in determining magnetic fields induced by surface waves on a deep ocean. Beal and Weaver [1970] also investigate magnetic fields produced by internal waves propagating along a sharp thermocline. Both papers, however, neglect the electric field.

Measurements by Maclure, et al. [1964] of magnetic fields induced at the surface by ocean swell agree with estimates made by Weaver. Measurements of Russian workers [Kozlov, et al., 1971; Kravtsov, et al., 1971, and Groskaya, et al., 1972] indicate that sea waves approaching a shoreline produce appreciable magnetic fields. Indeed, magnetic field magnitudes per unit wave height appear to be anomalously large.

At present, then, the understanding of electric and magnetic effects of steady ocean currents and progressive waves provide a means of investigating simple flow fields in an ocean. Flow fields in an ocean, however, are commonly in a confused state, and statistical methods are required to describe them [Longuet-Higgins, 1957]. The energy spectrum of a random wave field then provides a means of describing its statistical properties, and conversely, measurement of statistical properties, in principle, provides a means of determining energy spectra.

Our overall purpose is twofold: (1) to establish a correspondence between noise spectra of electromagnetic fields induced by ocean waves and energy spectra of both surface and internal waves, and (2) to suggest suitable procedures for determining wave spectra from measurements of electromagnetic noise spectra. Correspondence between electromagnetic noise spectra and ocean wave spectra is provided by a transfer function, which is the electromagnetic field induced by a progressive ocean wave of unit wave height.

Ideally, noise spectra of induced magnetic and/or electric fields are simply the product of the squared modulus of the transfer function and ocean wave energy spectra, because induced fields are responses of a linear network — the Earth's magnetic field. Measurements must contend with electromagnetic noise produced by ionospheric and/or geologic sources as well as separate noise spectra produced by surface and internal waves. Consequently, properly designed experiments lead to more complicated relations between spectra and thus require rather complete information on the transfer function, for both design and interpretation.

Our immediate purpose herein, then, is to develop a complete description of electromagnetic fields induced by both surface and internal ocean waves. A subsequent paper presents correspondences between electromagnetic noise spectra and ocean wave spectra.

We begin by presenting in Section II a general solution for the electromagnetic field induced by an irrotational flow field using Ampere's law and Faraday's law and show that fields are determined by an electromagnetic potential function and a velocity potential function. We then determine solutions corresponding to progressive waves in a horizontally stratified ocean.

To develop insight, we first investigate fields produced by progressive waves in a deep ocean in Section III and then consider fields produced by progressive waves in shallow seas in Section IV. In each case, we present fields produced by both surface and internal waves in both polar and equatorial regions. Finally, we give complete expressions for electromagnetic potential functions corresponding to surface and internal waves in the Appendix.

II. ELECTROMAGNETIC FIELDS INDUCED BY OCEAN WAVES

Sea water moving across the Earth's magnetic field induces an electric current in the sea that generates an electromagnetic field characteristic of the velocity field in the sea. Motion of sea water with velocity \vec{v} across the Earth's constant magnetic field, \vec{B} , induces an electric field, $\vec{E}_1 = \vec{v} \times \vec{B}$. The electric current, \vec{J} , produced in the sea is expressed in MKS units as

$$\vec{J} = \sigma (\vec{E} + \vec{E}_1) \quad , \quad (1)$$

where \vec{E} is the electric field in a stationary frame of reference and σ , the electrical conductivity, which is about 4 mhos/m for sea water. Because phase speeds of ocean waves are much less than the speed of light, displacement currents in the sea are negligible, and the magnetic field, \vec{b} , of the induced current is determined by Ampere's law in the form

$$\vec{v} \times \vec{b} = \mu_0 \vec{J} \quad , \quad (2)$$

where $\mu_0 = 4\pi \times 10^{-7}$ henry/m. A second order contribution to the induced current proportional to $\vec{v} \times \vec{b}$ is negligible, since amplitudes of induced magnetic fields are several orders of magnitude smaller than the Earth's field. Finally, electric and magnetic fields are related by Faraday's law, so that

$$\vec{v} \times \vec{E} = - \frac{\partial \vec{b}}{\partial t} \quad , \quad (3)$$

Equations (1), (2), and (3), together with appropriate boundary conditions, determine the electromagnetic field, \vec{E} and \vec{b} , generated by sea water motion having a velocity field \vec{v} . Because the conductivity of sea water is small, the Lorentz body force, $\vec{J} \times \vec{B}$, acting on the fluid as a result of the induced current is negligibly small compared to pressure and buoyancy forces. Consequently, hydromagnetic effects are absent.

For our purposes, sea water flow fields are adequately described by irrotational motion of an incompressible and inviscid fluid, so that the velocity field is the gradient of a potential function, $\vec{v} = -\vec{\nabla} \Psi$, and both its divergence and vorticity vanish.* The induced electric field, then, is solenoidal and is expressed in terms of the potential function as

$$\vec{E}_i = -\vec{\nabla} \times \Psi \vec{B} \quad (4)$$

In a sea having a uniform electrical conductivity, the divergence of \vec{E} also vanishes, so that all vector fields are solenoidal.

By taking the curl of both Equations (2) and (3), we obtain the expressions

$$\nabla^2 \vec{E} - \mu_0 \sigma \frac{\partial \vec{E}}{\partial t} = \mu_0 \sigma \frac{\partial \vec{E}_i}{\partial t} \quad (5a)$$

and

$$\nabla^2 \vec{b} - \mu_0 \sigma \frac{\partial \vec{b}}{\partial t} = -\mu_0 \sigma \vec{v} \times \vec{E}_i \quad (5b)$$

relating the solenoidal field vectors \vec{E} and \vec{b} to the induced electric field \vec{E}_i .

* Vorticity is important in tidal motions, because Coriolis forces then influence flow fields.

A. PARTICULAR SOLUTION

A particular electromagnetic field, \vec{E}_p and \vec{b}_p , satisfying Equations (5a) and (5b), is given by

$$\vec{E}_p = -\vec{E}_i \quad (6)$$

and

$$\frac{\partial \vec{b}_p}{\partial t} = \vec{\nabla} \times \vec{E}_i, \quad (7)$$

since $\nabla^2 \vec{E}_i$ vanishes. The particular fields are expressed in terms of the velocity potential function as

$$\vec{E}_p = \vec{\nabla} \times \psi \vec{B} \quad (8a)$$

and

$$\frac{\partial \vec{b}_p}{\partial t} = -\vec{\nabla} (\vec{B} \cdot \vec{\nabla} \psi) \quad (8b)$$

B. HOMOGENEOUS SOLUTION

Because a solenoidal vector field is determined by two scalar functions [Morse and Feshbach, 1953], we express the electric field, \vec{E}_h , that satisfies the homogeneous form of Equation (5a) in terms of two scalar functions, Φ_1 and Φ_2 , and a unit vector \hat{z} directed vertically downward in the form

$$\vec{E}_h = \vec{\nabla} \times (\Phi_1 \hat{z} + \hat{z} \times \vec{\nabla} \Phi_2), \quad (9a)$$

where both Φ_1 and Φ_2 satisfy the expression

$$\nabla^2 \Phi_i - \mu_0 \sigma \frac{\partial \Phi_i}{\partial t} = 0 \quad (9b)$$

The corresponding magnetic field, \vec{b}_h , is determined by

$$\frac{-\partial \vec{b}_h}{\partial t} = \vec{\nabla} \times \vec{E}_h \quad (10a)$$

so that

$$\frac{\partial \vec{b}_h}{\partial t} = -\vec{\nabla} (\hat{z} \cdot \vec{\nabla} \Phi_1) + \mu_0 \sigma \frac{\partial}{\partial t} (\Phi_1 \hat{z} + \hat{z} \times \vec{\nabla} \Phi_2) \quad (10b)$$

The function Φ_1 generates a transverse electric type field, so called because the corresponding electric field vector is transverse to the gradient direction, and Φ_2 generates a so-called transverse magnetic type field.

Above the ocean surface, conductivity vanishes. As a result, the transverse magnetic component reduces to an electrostatic type field; fields above the surface are given by

$$\vec{E}_a = \vec{\nabla} \times \Phi_{a1} \hat{z} + \vec{\nabla} \Phi_{a2} \quad (11a)$$

and

$$\frac{\partial \vec{b}_a}{\partial t} = -\vec{\nabla} (\hat{z} \cdot \vec{\nabla} \Phi_{a1}) \quad (11b)$$

where both Φ_{a1} and Φ_{a2} satisfy a Laplace equation

$$\nabla^2 \Phi_{ai} = 0 \quad (11c)$$

Since the particular solution vanishes above the ocean surface, the fields \vec{E}_a and \vec{b}_a are complete fields.

C. GENERAL SOLUTION

Vertical electric currents in the sea are rapidly extinguished by accumulation of surface charge. Electric current is proportional to the homogeneous electric field, \vec{E}_h , so that the vertical component of \vec{E}_h vanishes. Consequently, the potential function ϕ_2 vanishes, and homogeneous fields are transverse electric type fields. Complete fields in the sea, \vec{E}_s and \vec{b}_s , which are a sum of particular and homogeneous fields, are then given by

$$\vec{E}_s = \vec{\nabla} \times (\phi_s \hat{z} + \psi \vec{B}) \quad (12a)$$

and

$$\frac{\partial \vec{b}_s}{\partial t} = -\vec{\nabla}(\vec{B} \cdot \vec{\nabla} \psi + \hat{z} \cdot \vec{\nabla} \phi_s) + \mu_0 \sigma \frac{\partial \phi_s}{\partial t} \hat{z}, \quad (12b)$$

where the potential function ϕ_s satisfies Equation (9b).

Above the ocean surface, complete fields are given by Equations (11a) and (11b). Below the ocean floor, electric and magnetic fields, \vec{E}_c and \vec{b}_c , are expressed as

$$\vec{E}_c = \vec{\nabla} \times \phi_c \hat{z} \quad (13a)$$

and

$$\frac{\partial \vec{b}_c}{\partial t} = -\vec{\nabla}(\hat{z} \cdot \vec{\nabla} \phi_c) + \mu_0 \sigma_c \frac{\partial \phi_c}{\partial t} \hat{z}, \quad (13b)$$

where

$$\nabla^2 \Phi_c - \mu_0 \sigma_c \frac{\partial \Phi_c}{\partial t} = 0 \quad (13c)$$

and σ_c is the conductivity of suboceanic strata.

D. PROGRESSIVE WAVE SOLUTION

As a first approximation, we consider oceans to be horizontally stratified and reckon the vertical coordinate, z , positive with increasing depth. We direct the horizontal x -axis northward and the y -axis eastward, so that the Earth's magnetic field vector lies in the x - z plane and is inclined at an angle ϕ to the x -axis.

Because we represent oceans as a composite of horizontal strata, we express each of the scalar potential functions that specify the electromagnetic field as a Fourier integral of a potential function corresponding to a horizontally progressing ocean wave having an angular frequency ω and horizontal wave vector \vec{k} . We express the velocity potential function, for example, as

$$\psi(z, \vec{r}, t) = \iint d\omega d\vec{k} \psi(z, \vec{k}, \omega) e^{i(\omega t - \vec{k} \cdot \vec{r})}, \quad (14)$$

where \vec{r} is a horizontal coordinate vector. The Fourier coefficient $\psi(z, \vec{k}, \omega)$ is the vertical profile of a wave progressing horizontally in a direction \vec{k} with an angular frequency ω .

Linear operators relate the electromagnetic field to potential functions. In order to determine the electromagnetic field produced by a specified flow field in the sea, then, we first relate Fourier coefficients of the electromagnetic field to those of potential functions. We determine the relation by finding the electromagnetic field produced

by a progressive wave in which potential functions have the form of the integrand of Equation (14).

For a progressive wave, the profile of the velocity field, $\vec{v}(z, \vec{k}, \omega)$, is a reduced gradient of the profile, $\psi(z, \vec{k}, \omega)$, of its potential function

$$\vec{v} = -\vec{\nabla}_r \psi, \quad (15a)$$

where the reduced gradient operator, $\vec{\nabla}_r$, is defined by

$$\vec{\nabla}_r \equiv \hat{z} \frac{d}{dz} - i\vec{k}. \quad (15b)$$

Since the velocity potential function satisfies a Laplace equation, its profile in a progressive wave satisfies the Helmholtz equation

$$\frac{d^2 \psi}{dz^2} - k^2 \psi = 0. \quad (15c)$$

To facilitate further calculation and interpretation, we express \vec{v} as a sum of circularly polarized components in the form

$$\vec{v} = \frac{k\psi}{\sqrt{2}} [(1+p)\hat{v} - (1-p)\hat{v}^*], \quad (16a)$$

where

$$p(z, \vec{k}, \omega) = -\frac{1}{k} \frac{d \ln \psi}{dz}, \quad (16b)$$

$$\hat{v} = \frac{1}{\sqrt{2}} (\hat{z} + i\vec{k}), \quad (16c)$$

\hat{k} is a unit vector in the direction of wave propagation, k is a wave number, and \hat{v}^* is the complex conjugate of \hat{v} . The unit vector \hat{v} has the convenient property that $\hat{v} \times \hat{n} = i\hat{v}$, where $\hat{n} = \hat{z} \times \hat{k}$, so that $\hat{v} \cdot \hat{n} = 0$. Circular polarization of \hat{v} is left-handed with respect to \hat{n} , and that of its complex conjugate \hat{v}^* is right-handed.

The velocity vector of a progressive wave, then, is elliptically polarized in a vertical plane containing the wave vector. Eccentricity of the ellipse and sense of rotation with respect to the direction of the unit vector \hat{n} , normal to the plane of polarization, are determined by the value of the function $p(z, \vec{k}, \omega)$, which we call the polarization coefficient.

From Expression (12a) that relates the electric field in the sea to a velocity potential and a potential function ϕ_s , satisfying Equation (9b), we find that the electric field profile, $\vec{\epsilon}_s(z, \vec{k}, \omega)$, of a progressive wave is given by the expression

$$\vec{\epsilon}_s = ik \phi_s \hat{n} - \vec{v} \times \vec{B} \quad , \quad (17a)$$

where $\phi_s(z, \vec{k}, \omega)$ is the progressive wave profile of the potential function ϕ_s and so satisfies the Helmholtz equation

$$\frac{d^2 \phi_s}{dz^2} - \alpha^2 \phi_s = 0 \quad , \quad (17b)$$

with $\alpha^2 = k^2 + i\mu_0 \sigma \omega$. By expressing the vector product $\vec{v} \times \vec{B}$ as a sum of components along and transverse to the unit vector \hat{n} , we write Equation (17a) as a sum of transverse electric and electrostatic type fields in the form

$$\vec{\epsilon}_s = [ik\phi_s + \vec{B} \cdot (\vec{\nu} \times \hat{n})]\hat{n} - (\vec{B} \cdot \hat{n})(\vec{\nu} \times \hat{n}) . \quad (18a)$$

The profile of the electric current produced in the sea by a progressive wave is simply

$$\vec{j}_s = ik\sigma\phi_s\hat{n} . \quad (18b)$$

By taking the curl of the electric field, we obtain the expression

$$i\omega\vec{\beta}_s = \hat{n} \times \vec{\nabla}_r [ik\phi_s + \vec{B} \cdot (\vec{\nu} \times \hat{n})] , \quad (19)$$

for the profile of the magnetic field.

By writing the reduced gradient of ϕ_s in terms of circularly polarized components, we express magnetic and electric field profiles in terms of circularly polarized components as

$$\begin{aligned} \left(\frac{\omega}{k}\right)\vec{\beta}_s &= ik\left[\frac{\phi_s}{\sqrt{2}}(1 + p_s) + \psi(1 + p)(\vec{B} \cdot \hat{\nu})\right]\hat{\nu} \\ &+ ik\left[\frac{\phi_s}{\sqrt{2}}(1 - p_s) + \psi(1 - p)(\vec{B} \cdot \hat{\nu}^*)\right]\hat{\nu}^* \end{aligned} \quad (20a)$$

and

$$\begin{aligned} \vec{\epsilon}_s &= ik\left\{\phi_s + \frac{\psi}{\sqrt{2}}[(1 + p)(\vec{B} \cdot \hat{\nu}) + (1 - p)(\vec{B} \cdot \hat{\nu}^*)]\right\}\hat{n} \\ &- \frac{ik\psi}{\sqrt{2}}(\vec{B} \cdot \hat{n})[(1 + p)\hat{\nu} + (1 - p)\hat{\nu}^*] . \end{aligned} \quad (20b)$$

We observe from Equation (20b) that the electrostatic part of the electric field vanishes in polar regions where the Earth's magnetic field is nearly vertical so that $\vec{B} \cdot \hat{n}$ vanishes. The field is then a pure transverse electric type field. In equatorial regions, the field is a pure electrostatic type field when $\vec{B} = B\hat{n}$, so that $\vec{B} \cdot \hat{n}$ and hence ϕ_s vanish. We also note that the ratio of the transverse component of the electric field to the vertical component of the magnetic field is the phase speed of an ocean wave; namely,

$$\frac{\vec{\epsilon}_s \cdot \hat{n}}{\vec{\beta}_s \cdot \hat{z}} = \frac{\omega}{k} \quad (20c)$$

In conducting strata below the oceans, the velocity potential vanishes, and electric and magnetic fields are transverse electric type fields. Their profiles are expressed by Equations (20b) and (20a) with $\psi = 0$ and ϕ_s replaced by a potential profile ϕ_c . The profile ϕ_c satisfies a Helmholtz equation like Equation (17b) with a constant, α_c^2 , corresponding to the conductivity of suboceanic strata.

Above the ocean surface, the electric and magnetic field profiles, $\vec{\epsilon}_a$ and $\vec{\beta}_a$, are given in terms of potential profiles ϕ_{a1} and ϕ_{a2} by the expressions

$$\vec{\epsilon}_a = ik\phi_{a1}\hat{n} + \vec{\nabla}_r\phi_{a2} \quad (21a)$$

and

$$\left(\frac{\omega}{k}\right)\vec{\beta}_a = \hat{n} \times \vec{\nabla}_r\phi_{a1} \quad (21b)$$

where both ϕ_{a1} and ϕ_{a2} satisfy the equation

$$\frac{d^2 \phi_{ai}}{dz^2} - k^2 \phi_{ai} = 0 . \quad (21c)$$

Because fields must vanish far above the surface, potential profiles are of exponential form, so that

$$\vec{\nabla}_r \phi_{ai} = k \phi_{ai} \sqrt{2} \hat{\nu}^* . \quad (21d)$$

Field profiles above the surface are expressed in terms of circularly polarized components as

$$\vec{\epsilon}_a = ik \phi_{a1} \hat{n} + \sqrt{2} k \phi_{a2} \hat{\nu}^* \quad (22a)$$

and

$$\left(\frac{\omega}{k}\right) \vec{\beta}_a = i \sqrt{2} k \phi_{a1} \hat{\nu}^* . \quad (22b)$$

Whatever the polarization of the velocity field, the magnetic field produced above the surface by a progressive wave is circularly polarized with a right-handed sense of rotation.

In each horizontal layer (air, strata within a sea, and sub-oceanic strata), specification of two arbitrary constants determines the electromagnetic field produced by a progressive wave. Requiring continuity of horizontal components of electric and magnetic field vectors at interfaces together with requiring fields to vanish far enough

above and below an ocean specify the two constants in each layer.

Further description of the field, then, requires specifying a model to represent an ocean. In order to develop insight, we begin with the simplest stratification model — a homogeneous, deep ocean — and proceed to multilayered models representing shallow, stratified seas.

III. ELECTROMAGNETIC FIELDS INDUCED BY PROGRESSIVE WAVES IN A DEEP OCEAN

In this section, we describe electromagnetic fields produced by progressive waves in an ocean that is several wave lengths deep ($kD \gg 1$). We first consider surface waves on an homogeneous ocean and then internal waves propagating along a sharp thermocline. In each case, we suppose that wave amplitudes are much smaller than a wavelength and so restrict consideration to a linear regime.

A. SURFACE WAVES

In a deep ocean, the velocity potential profile, ψ , and the electromagnetic potential profile ϕ_s decrease exponentially with depth as e^{-kz} and $e^{-\alpha z}$, respectively, since all fields vanish at great depths. The polarization coefficient of the velocity profile is unity, and $p_s = \alpha/k$, where

$$\left(\frac{\alpha}{k}\right)^2 = 1 + i\delta^2 \quad (23a)$$

with

$$\delta^2 = \frac{u_0 \sigma \omega}{k^2} \quad (23b)$$

The quantity $\delta/\sqrt{2}$ is the ratio of wavelength of an ocean wave to wavelength of an electromagnetic wave in the sea, λ_e , where $\lambda_e = 2\pi(2/\mu_0 \sigma \omega)^{1/2}$ [Kraichman, 1970].

From Equations (20a) and (20b), we then find that electric and magnetic field profiles in a deep ocean are given by the expressions

$$\begin{aligned}\vec{\epsilon}_s &= ik [\phi_0 e^{-\alpha z} + \psi_0 \sqrt{2} (\vec{B} \cdot \hat{v}) e^{-kz}] \hat{n} \\ &- ik \psi_0 (\vec{B} \cdot \hat{n}) e^{-kz} \sqrt{2} \hat{v}\end{aligned}\quad (24a)$$

and

$$\begin{aligned}\left(\frac{\omega}{k}\right) \vec{\beta}_s &= \frac{ik}{\sqrt{2}} \left[\phi_0 \left(\frac{\alpha}{k} + 1 \right) e^{-\alpha z} + 2\psi_0 \sqrt{2} (\vec{B} \cdot \hat{v}) e^{-kz} \right] \hat{v} \\ &- \frac{ik}{\sqrt{2}} \phi_0 \left(\frac{\alpha}{k} - 1 \right) e^{-\alpha z} \hat{v}^*,\end{aligned}\quad (24b)$$

where ψ_0 and ϕ_0 are values of ψ and ϕ_s at the surface, $z = 0$. The profile of the current induced in the sea, \vec{j}_s , is expressed as

$$\vec{j}_s = \sigma ik \phi_0 e^{-\alpha z} \hat{n} \quad (24c)$$

Above the surface ($z < 0$), field profiles are expressed in terms of two constants, A_0 and A_1 , as

$$\vec{\epsilon}_a = ik e^{kz} (A_0 \hat{n} - iA_1 \sqrt{2} \hat{v}^*) \quad (25a)$$

and

$$\left(\frac{\omega}{k}\right) \vec{\beta}_a = ik A_0 e^{kz} \sqrt{2} \hat{v}^* \quad (25b)$$

By imposing continuity of horizontal field components at the surface, we obtain the expressions

$$\phi_0 = - \left(\frac{2k}{\alpha + k} \right) \psi_0 \sqrt{2} (\vec{B} \cdot \hat{\nu}) , \quad (26a)$$

$$A_0 = \left(\frac{\alpha - k}{\alpha + k} \right) \psi_0 \sqrt{2} (\vec{B} \cdot \hat{\nu}) , \quad (26b)$$

and

$$A_1 = i \psi_0 (\vec{B} \cdot \hat{n}) \quad (26c)$$

relating the constants ϕ_0 , A_0 , and A_1 to ψ_0 . For ocean wave amplitudes that are much less than wavelengths, the profile of wave amplitude, ξ , is expressed in terms of the velocity potential profile by the kinematical relation

$$i\omega\xi = k\psi , \quad (27a)$$

so that wave height at the surface, ξ_0 , of a progressive wave in a deep ocean is given in terms of ψ_0 by the expression

$$i\omega\xi_0 = k\psi_0 . \quad (27b)$$

Fields in the sea, then are proportional to surface wave heights and are expressed by

$$\vec{\epsilon}_s = -\omega \xi_0 e^{-kz} \sqrt{2} \left\{ \left[1 - \left(\frac{2k}{\alpha + k} \right) e^{-(\alpha - k)z} \right] (\vec{B} \cdot \hat{v}) \hat{n} - (\vec{B} \cdot \hat{n}) \hat{v} \right\} \quad (28a)$$

and

$$\vec{\beta}_s = -k \xi_0 e^{-kz} 2(\vec{B} \cdot \hat{v}) \left\{ \left[1 - e^{-(\alpha - k)z} \right] \hat{v} + \left(\frac{\alpha - k}{\alpha + k} \right) e^{-(\alpha - k)z} \hat{v}^* \right\} \quad (28b)$$

below the surface ($z > 0$) and by

$$\vec{\epsilon}_a = -\omega \xi_0 e^{kz} \sqrt{2} \left[\left(\frac{\alpha - k}{\alpha + k} \right) (\vec{B} \cdot \hat{v}) \hat{n} + (\vec{B} \cdot \hat{n}) \hat{v}^* \right] \quad (28c)$$

and

$$\vec{\beta}_a = -k \xi_0 e^{kz} 2(\vec{B} \cdot \hat{v}) \left(\frac{\alpha - k}{\alpha + k} \right) \hat{v}^* \quad (28d)$$

above the surface ($z < 0$). The profile of the current induced in the sea is given by

$$\vec{j}_s = \sigma \omega \xi_0 e^{-kz} \left(\frac{2k}{\alpha + k} \right) e^{-(\alpha - k)z} \sqrt{2} (\vec{B} \cdot \hat{v}) \hat{n} \quad (29)$$

Bernoulli's equation in linearized form [Lamb, 1932] gives the relation

$$i\omega\xi_0 = \frac{2}{g} \psi_0 \quad (30a)$$

between wave height and the velocity potential profile at a free surface, where $g = 9.8 \text{ m/sec}^2$. The kinematical relation given by Equation (27b) together with Equation (30a), then, give the dispersion law, $\omega^2 = gk$, for surface waves in a deep ocean. By using the dispersion law, we express the square of the ratio of ocean wavelength to electromagnetic wavelength as

$$\frac{\delta^2}{2} = \frac{\mu_0 \sigma}{2k} \left(\frac{g}{k} \right)^{1/2}, \quad (30b)$$

so that

$$\frac{\delta^2}{2} \cong (5 \times 10^{-7}) \lambda^{3/2} \quad (30c)$$

where λ is wavelength measured in meters. For ocean wavelengths less than a few kilometers, corresponding to wave periods less than a few tens of seconds, wavelengths of ocean waves in a deep ocean are much less than those of electromagnetic waves.* The ratio α/k , determined by Equation (23a), is then given by

* In an ocean of depth D , phase speeds of surface waves are less than \sqrt{gD} [Lamb, 1932], so that $\delta^2/2 < 4\lambda \sqrt{gD} \times 10^{-7}$. Because ocean depths are of the order of 10 km at most, $\delta^2/2 < \lambda \times 10^{-4}$.

$$\frac{\alpha}{k} \approx 1 + i \frac{\delta^2}{2} \quad (30d)$$

to a good approximation.

Using the approximate form for the ratio α/k , we obtain first order expressions in δ^2 for fields in and above the ocean; namely,

$$\vec{\epsilon}_s = -\omega \xi_0 e^{-kz} \sqrt{2} \left[i \frac{\delta^2}{4} (1 + 2kz) (\vec{B} \cdot \hat{v}) \hat{n} - (\vec{B} \cdot \hat{n}) \hat{v} \right] \quad (31a)$$

$$\vec{\beta}_s = -ik \xi_0 e^{-kz} \frac{\delta^2}{2} (\vec{B} \cdot \hat{v}) (2kz \hat{v} + \hat{v}^*) \quad , \quad (31b)$$

$$\vec{\epsilon}_a = -\omega \xi_0 e^{kz} \sqrt{2} \left[i \frac{\delta^2}{4} (\vec{B} \cdot \hat{v}) \hat{n} + (\vec{B} \cdot \hat{n}) \hat{v}^* \right] \quad , \quad (31c)$$

and

$$\vec{\beta}_a = -ik \xi_0 e^{kz} \frac{\delta^2}{2} (\vec{B} \cdot \hat{v}) \hat{v}^* \quad . \quad (31d)$$

The induced current profile in the sea is expressed to first order as

$$\vec{j}_s = \sigma \omega \xi_0 e^{-kz} \left[1 - i \frac{\delta^2}{4} (1 + 2kz) \right] \sqrt{2} (\vec{B} \cdot \hat{v}) \hat{n} \quad . \quad (31e)$$

We note that the transverse electric component of the electric field and the magnetic field vanish as δ^2 becomes negligible, so that to zero order the field is an electrostatic-like field produced by surface charge. The zero order current is driven by the transverse component of the electric field induced by sea water motion. In polar regions, however, $\vec{B} \cdot \hat{n} \approx 0$, so that surface charge and hence the zero order electric field vanish, and only the transverse-electric type field remains.

From Equation (31b), we find that magnitudes of induced magnetic fields, to first order, are proportional to phase speeds of surface waves, since

$$k \delta^2 = \mu_0 \sigma \left(\frac{\omega}{k} \right) \quad (32a)$$

Similarly, magnitudes of the transverse-electric components of electric fields are proportional to the square of phase speeds. Because phase speeds of surface waves on a deep ocean are inversely proportional to frequency or, equivalently, to the square root of wave number, field magnitudes increase with decreasing frequency or wave number.

We remark that an increasing importance of magnetic induction effects with decreasing frequency is contrary to customary notions. Ordinarily, induction effects are more pronounced at higher frequencies. An increase in magnitude of induced fields with decreasing frequency does not continue indefinitely, however, because at zero frequency the sea is quiescent and induced fields vanish.

To illustrate the dependence of field magnitudes on wave number, we consider fields induced at the surface in polar regions. For ocean wavelengths that are much smaller than electromagnetic wavelengths, we find from Equation (31a) that the magnetic field strength induced at the surface by a one meter high wave in polar regions is given by

$$\frac{|\vec{b}_0|}{\xi_0} = B \left(\frac{\mu_0 \sigma}{2} \right) \sqrt{\frac{g}{2k}} \quad (32b)$$

and so increases with decreasing wave number. For ocean wavelengths

that are much greater than electromagnetic wavelengths, however, we find from Equation (28d) that magnetic field strength at the surface is proportional to wave number; namely

$$\frac{|\vec{b}_0|}{\xi_0} = B k \sqrt{2} \quad (32c)$$

and so decreases with decreasing wave number. In each case, corresponding electric field magnitudes are determined by the relation

$$|\vec{E}_0| = |\vec{b}_0| \sqrt{g/2k} \quad (32d)$$

Dependence of magnetic and electric field magnitudes on wave number is delineated in Figure 1 by the heavy solid and dashed curves, respectively. The light dashed lines are asymptotes determined by Equations (32b) and (32c). Curves in Figure 1 correspond to field magnitudes induced at the surface by a one meter high wave in polar regions, where the Earth's field strength is about 6.24×10^4 gammas [Chapman, 1962]. As is evident in Figure 1, field magnitudes attain maximum values at wavelengths near 10 km, where electromagnetic and ocean wavelengths are comparable. The magnitude of the magnetic field attains a maximum value of about 10 gamma/m, and the magnitude of the electric field, a value of about 1 microvolt/m².

Nonetheless, ocean wavelengths of several kilometers or greater are comparable to or exceed ocean depths, so that a deep ocean approximation no longer applies, and phase speeds of surface waves approach the limiting value \sqrt{gD} . Determination of field magnitudes induced by surface waves with wavelengths exceeding a few

kilometers, corresponding to wave periods exceeding a few tens of seconds, requires accounting for wave reflection from suboceanic strata — a topic that we consider in Section IV.

When a deep ocean approximation is adequate, however, ocean wavelengths are much less than electromagnetic wavelengths, so that Equations (31a) to (31d) adequately describe field profiles in a deep ocean. For purposes of discussion, we first consider polar regions. The magnetic field vector above the surface in polar regions is circularly polarized in a right-handed sense with respect to \hat{n} , and its magnitude decreases exponentially with altitude in accordance with the relation

$$|\vec{b}| = |\vec{b}_0| e^{kz} , \quad (33a)$$

with $|\vec{b}_0|$ determined by Equation (32b).

Below the surface, the magnetic field vector is elliptically polarized with the major axis of the ellipse aligned vertically. The sense of rotation is right-handed at depths less than $\lambda/4\pi$. At a depth of $\lambda/4\pi$, the field is linearly polarized in a vertical direction. Below a depth of $\lambda/4\pi$, the field is again elliptically polarized with the major axis of the ellipse aligned vertically, but the sense of rotation is left-handed. At great depths polarization becomes circular with a left-handed sense of rotation. The magnitude of the magnetic field below the surface decreases with depth according to the relation

$$|\vec{b}| = |\vec{b}_0| e^{-kz} \sqrt{1 + 4k^2 z^2} , \quad (33b)$$

Profiles of magnetic field strength and polarization induced in polar regions by a one meter high wave having a wavelength of 10 m are shown in Figure 2. Altitude and depth are measured in units of a wavelength.

In polar regions, surface charge vanishes, and electric fields are transverse electric type fields. The magnitude of the electric field decreases above the surface as

$$|\vec{E}| = |\vec{E}_0| e^{kz} \quad (34a)$$

and below the surface as

$$|\vec{E}| = |\vec{E}_0| (1 + 2kz) e^{-kz}, \quad (34b)$$

where the magnitude at the surface, $|\vec{E}_0|$, is given by

$$|\vec{E}_0| = \xi_0 B \left(\frac{\mu_0 \sigma}{4} \right) \left(\frac{g}{k} \right). \quad (34c)$$

The magnitude of the electric current density in polar region decreases exponentially with depth in accordance with the relation

$$|\vec{J}_0| = \sigma \omega \xi_0 B e^{-kz}. \quad (34d)$$

Magnitudes of current densities at the surface are inversely proportional to wave period and for a one meter high wave in polar regions, range from about 1.5 milliamperes/m² at a wave period of 1 sec to 0.015 milliamperes/m² at a period of 100 seconds.

In mid-latitude and equatorial regions, a circularly polarized electrostatic component, resulting from surface charge, is added to the electric field. The sense of rotation of the electrostatic component is right-handed with respect to \hat{n} above the surface and left-handed below the surface. Its magnitude decreases exponentially both above and below the surface as

$$|\vec{E}_e| = \omega \xi_0 \sqrt{2} |\vec{B} \cdot \hat{n}| e^{-k|z|} \quad (35a)$$

where

$$|\vec{B} \cdot \hat{n}| = B_p \frac{\cos \phi \sin \theta}{2} \sqrt{1 + 3 \sin^2 \Phi} \quad (35b)$$

B_p is the Earth's field strength in polar regions; θ , the angle between the direction of wave propagation and magnetic north; Φ , magnetic latitude, and $\tan \phi = 2 \tan \Phi$ relates dip angle, ϕ , and latitude. A one meter high wave propagating across magnetic meridians at the magnetic equator induces an electrostatic field strength at the surface of 0.28 millivolts/m for a wave period of 1 sec and 0.028 millivolts/m for a wave period of 10 sec.

In equatorial regions, magnitudes of the transverse electric component of the electric field and of the magnetic field are less than their magnitudes in polar regions by a factor of $\cos \theta/2$. At intermediate latitudes, magnitudes of surface fields are less than magnitudes in polar regions by a factor of

$$R = \frac{\cos \phi}{2} [(1 + 3 \sin^2 \Phi)(\tan^2 \phi + \cos^2 \theta)]^{1/2} \quad (35c)$$

Polarization of the magnetic field vector, however, is the same as in polar regions.

B. INTERNAL WAVES

For a deep ocean containing a sharp thermocline at a depth d , we express the profile of the velocity potential for a progressive wave as

$$\psi_1 = \psi_0 (\cosh kz - \eta^2 \sinh kz) \quad , \quad (36a)$$

above the thermocline ($0 \leq z \leq d$), and as

$$\psi_2 = \psi_d e^{-k(z-d)} \quad (36b)$$

below the thermocline ($z \geq d$), where ψ_0 and ψ_d are values of respective profiles at the surface ($z = 0$) and at the thermocline interface ($z = d$). Bernoulli's equation at a free surface, as given by Equation (30a), together with the kinematical relation expressed by Equation (27a) give the relation

$$\eta^2 = \omega^2 / gk \quad (37)$$

for the value of the polarization coefficient at the surface.

For surface waves, η^2 is unity, corresponding to the dispersion law $\omega^2 = gk$. For internal waves, however, η^2 is determined by the relation

$$\eta^2 = \frac{\Delta\rho/\rho_2}{\rho_1/\rho_2 + \coth kd} \quad , \quad (38a)$$

which assures continuity of pressure and the vertical component of velocity at a thermocline interface. Sea water density below a thermocline, ρ_2 , exceeds that above a thermocline, ρ_1 , by a small amount

$\Delta\rho$. To a good approximation,

$$\eta^2 = \frac{\Delta\rho/\rho}{1 + \coth kd} \quad (38b)$$

where $\Delta\rho/\rho$ is of the order of 10^{-3} [Phillips, 1969]. Requiring continuity of the vertical component of velocity alone at a thermocline gives the relation

$$-\psi_d = \psi_0 \sinh kd (1 - \eta^2 \coth kd) \quad (38c)$$

between values of respective profiles at the surface and thermocline interface. The horizontal component of velocity is discontinuous at a sharp thermocline.

We express the profile ϕ_s of the electromagnetic potential in terms of two constants, C_1 and C_2 , as the sum of exponentials

$$\phi_{s1} = C_1 e^{\alpha z} + C_2 e^{-\alpha z}, \quad (39a)$$

above the thermocline ($0 \leq z \leq d$), and in terms of a constant C_3 as

$$\phi_{s2} = C_3 e^{-\alpha(z-d)} \quad (39b)$$

below the thermocline ($z \geq d$), since ϕ_s vanishes at great depths. From Equations (20a) and (20b), we then obtain the expressions

$$\begin{aligned} \vec{\epsilon}_{s1} = ik \left\{ \phi_{s1} + \frac{\psi_0}{\sqrt{2}} \left[(1+\eta^2)(\vec{B} \cdot \hat{v}) e^{-kz} + (1-\eta^2)(\vec{B} \cdot \hat{v}^*) e^{kz} \right] \right\} \hat{n} \\ - \frac{ik\psi_0}{\sqrt{2}} (\vec{B} \cdot \hat{n}) \left[(1+\eta^2) e^{-kz} \hat{v} + (1-\eta^2) e^{kz} \hat{v}^* \right] \end{aligned} \quad (40a)$$

and

$$\begin{aligned} \left(\frac{\omega}{k} \right) \vec{\beta}_{s1} = \frac{ik}{\sqrt{2}} \left\{ C_1 \left(1 - \frac{\alpha}{k} \right) e^{\alpha z} + C_2 \left(1 + \frac{\alpha}{k} \right) e^{-\alpha z} \right. \\ + \left. \psi_0 (1+\eta^2) \sqrt{2} (\vec{B} \cdot \hat{v}) e^{-kz} \right\} \hat{v} \\ + \frac{ik}{\sqrt{2}} \left\{ C_1 \left(1 + \frac{\alpha}{k} \right) e^{\alpha z} + C_2 \left(1 - \frac{\alpha}{k} \right) e^{-\alpha z} \right. \\ + \left. \psi_0 (1-\eta^2) \sqrt{2} (\vec{B} \cdot \hat{v}^*) e^{kz} \right\} \hat{v}^* , \end{aligned} \quad (40b)$$

for electric and magnetic field profiles above the thermocline, and the expressions

$$\begin{aligned} \vec{\epsilon}_{s2} = ik \left[\phi_{s2} + \psi_d \sqrt{2} (\vec{B} \cdot \hat{v}) e^{-k(z-d)} \right] \hat{n} \\ - ik \psi_d \sqrt{2} (\vec{B} \cdot \hat{n}) e^{-k(z-d)} \hat{v} \end{aligned} \quad (40c)$$

and

$$\begin{aligned} \left(\frac{\omega}{k}\right) \vec{\beta}_{s2} = & \frac{ik}{\sqrt{2}} \left[C_3 \left(1 + \frac{\alpha}{k}\right) e^{-\alpha(z-d)} + 2\psi_d \sqrt{2} (\vec{B} \cdot \hat{v}) e^{-k(z-d)} \right] \hat{v} \\ & + \frac{ik}{\sqrt{2}} \left[C_3 \left(1 - \frac{\alpha}{k}\right) e^{-\alpha(z-d)} \right] \hat{v}^* , \end{aligned} \quad (40d)$$

for electric and magnetic field profiles below the thermocline. As before, field profiles above the surface are expressed in terms of two constants, A_0 and A_1 , by Equations (25a) and (25b).

By imposing continuity of horizontal components of fields both at the surface and at the thermocline, we express the constants C_1 , C_2 , C_3 , A_0 , and A_1 in terms of ψ_0 and η^2 . Because the resulting expressions are cumbersome, however, we list them in the Appendix. Here, we consider two approximations that allow considerable simplification in expressing field profiles. First, for internal waves, $\eta^2 \ll 1$, so we everywhere neglect η^2 as compared to unity. As a consequence, wave height at the free surface is negligibly small, and the potential function values ψ_0 and ψ_d are related to wave height at the thermocline, or thermocline displacement ξ_d , by the expression

$$i\left(\frac{\omega}{k}\right) \xi_d = \psi_d \cong -\psi_0 \sinh kd , \quad (41)$$

which we obtain from the kinematical relation and Equation (38c).

Second, the ratio of wavelength of an internal wave to wavelength of an electromagnetic wave is small in a deep ocean, as for surface waves. We express the square of the ratio in terms of phase speed of an internal wave as

$$\delta^2/2 = \frac{\mu_0 \sigma}{2k} \left(\frac{\omega}{k} \right) , \quad (42a)$$

and, from Equation (38b), we express the phase speed as

$$\frac{\omega}{k} = \left[\frac{g (\Delta \rho / \rho) d}{k d (1 + \coth k d)} \right]^{1/2} . \quad (42b)$$

Thus, internal wave phase speeds are less than $\sqrt{g(\Delta \rho / \rho) d}$, and so

$$\delta^2/2 < (4 \times 10^{-7}) \lambda \sqrt{g(\Delta \rho / \rho) d} , \quad (42c)$$

where λ is wavelength of an internal wave. Since thermocline depth cannot exceed ocean depths ($d < 10$ km) and $\Delta \rho / \rho$ is of the order of 10^{-3} ,

$$\delta^2/2 < (4 \times 10^{-6}) \lambda , \quad (42d)$$

so that the ratio is small for wavelengths less than a few tens of kilometers. For a deep ocean approximation, wavelengths are always of the order of or less than a few kilometers. Wavelengths of internal waves, then, are much smaller than wavelengths of electromagnetic waves in a deep ocean, and so to a good approximation

$$\alpha/k \approx 1 + i \delta^2/2 , \quad (42e)$$

as for surface waves.

By neglecting η^2 compared to unity and using the first order approximation for α/k , we express electric and magnetic field profiles to first order in δ^2 as

$$\vec{\epsilon}_a = \left(\frac{\omega}{k}\right) (\hat{z} \cdot \vec{\beta}_a) \hat{n} \quad (43a)$$

and

$$\vec{\beta}_a = ik\xi_d \frac{\delta^2}{2} \left(\frac{kd}{\sinh kd}\right) e^{kz} (\vec{B} \cdot \hat{v}^*) \hat{v}^* \quad (43b)$$

above the surface ($z \leq 0$); as

$$\vec{\epsilon}_{s1} = \left(\frac{\omega}{k}\right) (\hat{z} \cdot \vec{\beta}_{s1}) \hat{n} - \frac{\omega \xi_d}{2 \sinh kd} (\vec{B} \cdot \hat{n}) \sqrt{2} (e^{-kz} \hat{v} + e^{kz} \hat{v}^*) \quad (43c)$$

and

$$\begin{aligned} \vec{\beta}_{s1} = ik\xi_d \frac{\delta^2}{2} \left(\frac{\sinh kz}{\sinh kd}\right) & \left\{ \left[(\vec{B} \cdot \hat{v}^*) + (\vec{B} \cdot \hat{v}) \frac{kz e^{-kz}}{\sinh kz} \right] \hat{v} \right. \\ & \left. - \left[(\vec{B} \cdot \hat{v}) + (\vec{B} \cdot \hat{v}^*) \frac{k(z-d) e^{kz}}{\sinh kz} \right] \hat{v}^* \right\} \end{aligned} \quad (43d)$$

above the thermocline ($0 \leq z \leq d$); and as

$$\vec{\epsilon}_{s2} = \left(\frac{\omega}{k}\right) (\hat{z} \cdot \vec{\beta}_{s2}) \hat{n} + \omega \xi_d e^{-k(z-d)} \sqrt{2} (\vec{B} \cdot \hat{n}) \quad (43e)$$

and

$$\begin{aligned} \vec{\beta}_{s2} = ik\xi_d \frac{\delta^2}{2} e^{-k(z-d)} & \left\{ \left[(\vec{B} \cdot \hat{v}^*) + \left(\frac{kd e^{-kd}}{\sinh kd} - 2k(z-d) \right) (\vec{B} \cdot \hat{v}) \right] \hat{v} \right. \\ & \left. - (\vec{B} \cdot \hat{v}) \hat{v}^* \right\} \end{aligned} \quad (43f)$$

below the thermocline ($z \geq d$).

For purposes of discussion, we first consider polar regions. From Equation (43b), we find that the magnitude of the magnetic field produced at the surface by a thermocline displacement of one meter in polar regions is given by

$$\frac{|\vec{b}_o|}{\xi_d} = \frac{B}{\sqrt{2}} \left(\frac{\mu_o \sigma}{2} \right) \left[\frac{gd (\Delta \rho / \rho) kd e^{-kd}}{\sinh kd} \right]^{1/2} . \quad (44a)$$

The corresponding magnitude of the electric field at the surface is given by

$$\frac{|\vec{E}_o|}{\xi_d} = B \left(\frac{\mu_o \sigma}{4} \right) gd \left(\frac{\Delta \rho}{\rho} \right) e^{-kd} . \quad (44b)$$

Field magnitudes at the thermocline interface in polar regions are given by the expressions

$$\frac{|\vec{b}_d|}{\xi_d} = \frac{B}{\sqrt{2}} \left(\frac{\mu_o \sigma}{2} \right) \left[\frac{gd (\Delta \rho / \rho)}{kd (1 + \coth kd)} \right]^{1/2} \left[1 + \left(1 + \frac{kd e^{-kd}}{\sinh kd} \right)^2 \right]^{1/2} \quad (44c)$$

and

$$\frac{|\vec{E}_d|}{\xi_d} = B \left(\frac{\mu_o \sigma}{4} \right) gd (\Delta \rho / \rho) e^{-2kd} , \quad (44d)$$

which we obtain from Equations (43f) and (43e).

Magnitudes of the magnetic field induced at the surface and at a 100 meter deep thermocline by a thermocline displacement of one meter in polar regions are shown as functions of kd by the solid curves in Figure 3. Corresponding electric field magnitudes are delineated by dashed curves. We observe that field magnitudes increase as wave number decreases, as for surface waves. An eventual decrease in field magnitudes at still smaller wave numbers is not shown in Figure 3, as internal wavelengths then become comparable to or exceed ocean depths and a deep ocean approximation is no longer appropriate.*

For shallow thermoclines ($kd \leq 0.1$) in a deep ocean, field magnitudes are effectively independent of wave number, as is evident in Figure 3. And magnetic field magnitudes increase approximately as the square root of thermocline depth, as is evident from Equation (44a), because phase speeds of internal waves increase in proportion to the square root of thermocline depth for shallow thermoclines. Electric field magnitudes increase approximately in proportion to thermocline depth. Magnitude of the transverse electric field component is quite small, however, because phase speeds of internal waves are of the order of 1 m/sec or less.

For deep thermoclines ($kd \geq 1$), field magnitudes at the surface decrease rapidly with increasing wave number, so that fields induced by internal waves having wavelengths of the order of or less than a thermocline depth are small at the surface. Sea water above a thermocline, in effect, acts as a low pass filter. Nonetheless, we note that electric field magnitudes at the surface exceed those at the thermocline interface. Electric field strength increases above the thermocline because of changing polarization of the magnetic field.

* We consider wave reflection from suboceanic strata in Section IV.

Above the surface, the magnetic field vector is always circularly polarized in a right-handed sense with respect to \hat{n} , and its magnitude decreases exponentially with altitude. Below the surface, magnetic field profiles differ markedly for shallow and deep thermoclines.

Profiles of magnetic field magnitude and polarization produced by a thermocline displacement of one meter in polar regions are shown in Figure 4 for a shallow thermocline corresponding to $kd = 0.1$ and a thermocline depth of 100 m. Depth is measured in units of a thermocline depth.

We observe from the polarization diagram in Figure 4 that one polarization reversal occurs above the thermocline and two below. Polarization begins as circular with a right-handed sense of rotation at the surface, becomes linear with a vertical alignment at a depth of $d/4$, again becomes circular but with a left-handed sense of rotation at a depth of $d/2$, and is elliptical with a horizontal elongation and a left-handed sense of rotation at the thermocline depth, d . Below the thermocline, horizontal elongation of the polarization ellipse continues until the field becomes linearly polarized with a horizontal alignment at a depth of $5.5 d$. Thereafter, the sense of rotation again becomes right-handed, and horizontal elongation of the polarization ellipse lessens until polarization once again becomes circular at a depth of $10.5 d$. Vertical elongation then grows until polarization becomes linear with a vertical alignment at a depth of $15.5 d$. Thereafter, the sense of rotation becomes left-handed, elongation rapidly lessens, and so polarization is circular with a left-handed sense of rotation at great depths.

Because of frequent polarization changes with increasing depth, profiles of vertical and horizontal components of the magnetic field exhibit maxima and vanish at depths corresponding to appropriate states of linear polarization. We note, however, that the vertical component is constant above the thermocline, so that the electric field magnitude is also constant.

Profiles of magnetic field magnitude and polarization produced by a thermocline displacement of one meter in polar regions are shown in Figure 5 for a deep thermocline corresponding to $kd=4$ and a thermocline depth of 100 m. We observe from the polarization diagram in Figure 5 that one polarization reversal occurs at the thermocline, one above the thermocline, and one below the thermocline. Because the magnetic field is linearly polarized with a horizontal alignment at the thermocline and circularly polarized at the surface, the vertical component of the field vanishes at the thermocline and increases above the thermocline. As a result, the electric field strength at the surface exceeds that at the thermocline, as we noted previously.

In equatorial regions, magnitudes of the magnetic field and transverse component of the electric field at the surface are less than surface magnitudes in polar regions by a factor of $\cos \theta/2$, where θ is the angle between the direction of internal wave propagation and magnetic north. Furthermore, the electric field contains an electrostatic component that is linearly polarized at the surface with a vertical alignment and circularly polarized at and below the thermocline, with a left-handed sense of rotation. Magnitudes of the electrostatic components are proportional to $\sin \theta$.

Magnetic field magnitudes produced at the surface and at a 100 meter deep thermocline by a thermocline displacement of one meter

propagating along magnetic meridians ($\theta=0$) in equatorial regions are shown as functions of kd by the solid curves in Figure 6. Magnitudes of the electrostatic component of the electric field corresponding to propagation across magnetic meridians ($\theta=\pi/2$) in equatorial regions are delineated by dashed curves in Figure 6.

We observe that magnetic field strengths at the surface and thermocline interface are equal for shallow thermoclines in equatorial regions. Magnitude of the electrostatic field at the surface decreases as kd increases, but magnitude of the electrostatic field at the thermocline interface increases as kd increases.

Profiles of magnetic field magnitude and polarization produced by a thermocline displacement of one meter propagating along magnetic meridians in equatorial regions are shown in Figure 7a for a shallow thermocline, corresponding to $kd=0.1$ and a thermocline depth of 100 m. Figure 7b illustrates magnitude and polarization profiles for the electrostatic field corresponding to propagation across magnetic meridians. For a shallow thermocline we note that field magnitudes are constant above the thermocline. The electrostatic field, however, vanishes above the surface because internal waves produce negligible surface displacements. Polarization of the magnetic field is like that of a surface wave, as is that of the electrostatic field below the thermocline.

Magnitude and polarization profiles of magnetic and electrostatic fields corresponding to a deep thermocline, $kd=4$, are shown in Figures 8a and 8b, respectively. For a deep thermocline, we note that magnetic field profiles are nearly symmetrical with respect to the thermocline interface. Because the electrostatic field vanishes above the surface, its polarization above the thermocline becomes

linear with a vertical alignment at surface. The polarization below the thermocline, however, is circular with a left-handed sense of rotation.

At midlatitudes, magnetic and transverse electric field magnitudes at the surface are less than those in polar regions by the factor R given by Equation (35c). Similarly, magnitude of the electrostatic field component at the surface is proportional to $|\vec{E} \cdot \hat{n}|$, which is expressed as a function of latitude and direction of wave propagation by Equation (35b). Polarization of field profiles, however, also change with latitude. We forego describing polarization changes with latitude, but remark that axes of polarization ellipses are no longer aligned vertically and horizontally.

IV. ELECTROMAGNETIC FIELDS INDUCED BY PROGRESSIVE WAVES IN SHALLOW SEAS

In this section, we describe electromagnetic fields produced by progressive waves in a sea that is shallower than a wavelength ($kD \leq 1$). We again suppose that wave amplitudes are much smaller than a wavelength. As in Section III, we first consider surface waves on a homogeneous ocean and then internal waves propagating on a sharp thermocline at a depth d .

Information on suboceanic conductivity profiles is sparse. Conductivity of the Earth's crust below the oceans is much less than that of sea water. Conductivity increases with depth within the Earth's mantle below the crust and becomes much greater than that of sea water. Estimates of the extent of the poorly conducting crustal layer beneath the oceans range from a few tens of kilometers to a few hundreds of kilometers[Cox, et al., 1970].

To account for reflections from suboceanic strata, we choose a two layer model to describe conductivity profiles beneath the ocean floor. We suppose that a poorly conducting layer, extending to a depth $D+h$, rests on a highly conducting layer extending indefinitely below the poorly conducting layer.

A. SURFACE WAVES

We express the profile of the velocity potential for a progressive surface wave as

$$\psi = \psi_0 (\cosh kz - \eta^2 \sinh kz) \quad (45a)$$

where ψ_0 is the value of the profile at the surface. As before, Bernoulli's equation together with the kinematical relation give the relation

$$\eta^2 = \omega^2/gk \quad (45b)$$

for the value of the polarization coefficient at the surface. Because the vertical component of velocity vanishes at the ocean floor,

$$\eta^2 = \tanh kD, \quad (45c)$$

which is the dispersion relation for surface waves on an ocean of depth D .

We express the profile of the electromagnetic potential within the sea as the sum of exponentials given by Equation (39a). Consequently, electric and magnetic fields within the sea are expressed by Equations (40a) and (40b) with η^2 given by Equation (45c). As always, field profiles above the surface are expressed by Equations (25a) and (25b).

The velocity potential vanishes in suboceanic strata, and the magnetic field profile is expressed by

$$\begin{aligned} \left(\frac{\omega}{k}\right) \vec{\beta}_{c1} = & \frac{ik}{\sqrt{2}} C_3 \left\{ \left[\left(\frac{\alpha_1}{k} + 1 \right) e^{-\alpha_1(z-D-\tilde{h})} \right. \right. \\ & + \left. \left(\frac{\alpha_1}{k} - 1 \right) e^{\alpha_1(z-D-\tilde{h})} \right] \hat{v} \\ & \left. - \left[\left(\frac{\alpha_1}{k} - i \right) e^{-\alpha_1(z-D-\tilde{h})} + \left(\frac{\alpha_1}{k} + 1 \right) e^{\alpha_1(z-D-\tilde{h})} \right] \hat{v}^* \right\} \quad (46a) \end{aligned}$$

in the poorly conducting layer ($D \leq z \leq D+h$), and by

$$\left(\frac{\omega}{k}\right) \vec{\beta}_{c2} = \frac{ik\sqrt{2}}{\left(\frac{\alpha_2}{\alpha_1} + 1\right)} C_3 e^{\alpha_1(\tilde{h}-h)} e^{-\alpha_2(z-D-h)} \left[\left(\frac{\alpha_2}{k} + 1\right) \hat{v} - \left(\frac{\alpha_2}{k} - 1\right) \hat{v}^* \right] \quad (46b)$$

in the highly conducting layer, $z \geq D+h$. The complex length \tilde{h} is determined by the relation

$$e^{-2\alpha_1(\tilde{h}-h)} = \frac{\alpha_2 - \alpha_1}{\alpha_2 + \alpha_1}, \quad (46c)$$

where α_1 corresponds to the conductivity of the poorly conducting layer and α_2 , to the conductivity of the highly conducting layer. The electric field in suboceanic strata is a transverse electric type field, and its profile in each layer is expressed as

$$\vec{E}_{cj} = \frac{\omega}{k} (\hat{z} \cdot \vec{\beta}_{cj}) \hat{n} \quad (46d)$$

We note that as conductivity of the highly conducting layer becomes indefinitely large and that of the poorly conducting layer becomes indefinitely small, the length \tilde{h} approaches h and α_1 approaches k . Perfect reflection then occurs at the highly conducting layer, and losses within the poorly conducting layer vanish. Furthermore, for ocean wavelengths that are much less than the extent of the poorly conducting layer ($kh \gg 1$), conductivity profiles of suboceanic strata are

well approximated by a vacuum region of indefinite extent below the ocean floor.

By requiring continuity of horizontal components of electric and magnetic fields at the surface and bottom of the sea, we obtain expressions for the constants determining electromagnetic potentials. Complete expressions for the electromagnetic potential in each layer are listed in the Appendix. Here, we express fields to first order in δ^2 .

From Equations (42a) and (45c), we find that the square of the ratio of ocean wavelength to electromagnetic wavelength is expressed in terms of wave number of a surface wave as

$$\frac{\delta^2}{2} = \frac{\mu_0 \sigma}{2k} \left[gD \frac{\tanh kD}{kD} \right]^{1/2}. \quad (47)$$

The quantity $\delta^2/2$ is shown as a function of kD and D/λ in Figure 9 for four ocean depths. As we noted in Section III, $\delta^2/2$ is always small for wavelengths less than an ocean depth. We also observe that $\delta^2/2$ is small for wavelengths ten times an ocean depth provided ocean depths are less than a kilometer, which we refer to as shallow seas.

For shallow seas then, we again express the ratio α/k to first order in δ^2 as given by Equation (30d). Furthermore, because the thickness, h , of the low conductivity layer beneath the oceans exceeds a few tens of kilometers, we represent strata below shallow seas as a vacuum region of indefinite extent.

We express magnetic field profiles in shallow seas to first order in δ^2 , then as

$$\vec{\beta}_a = -i\xi_0 \frac{k\delta^2}{2} \left[(\vec{B} \cdot \hat{v}) + \frac{kD e^{-kD}}{\sinh kD} (\vec{B} \cdot \hat{v}^*) \right] e^{kz} \hat{v}^* \quad (48a)$$

above the surface ($z \leq 0$), and as

$$\begin{aligned} \vec{\beta}_s = \frac{-i\xi_0}{\sinh kD} \frac{k\delta^2}{2} & \left\{ \left[(\vec{B} \cdot \hat{v}^*) e^{-kD} \sinh kz + (\vec{B} \cdot \hat{v}) kz e^{k(D-z)} \right] \right. \\ & \left. + \left[(\vec{B} \cdot \hat{v}) \sinh k(D-z) + (\vec{B} \cdot \hat{v}^*) k(D-z) e^{-k(D-z)} \right] \hat{v}^* \right\} \quad (48b) \end{aligned}$$

within the sea ($0 \leq z \leq D$). Corresponding electric field profiles are given by

$$\vec{\epsilon}_a = \left(\frac{\omega}{k} \right) (\hat{z} \cdot \vec{\beta}_a) \hat{n} - \omega \xi_0 (\vec{B} \cdot \hat{n}) e^{kz} \sqrt{2} \hat{v}^* \quad (48c)$$

above the surface and by

$$\begin{aligned} \vec{\epsilon}_s = \left(\frac{\omega}{k} \right) (\hat{z} \cdot \vec{\beta}_s) \hat{n} + \frac{\omega \xi_0}{\sinh kD} \frac{(\vec{B} \cdot \hat{n})}{\sqrt{2}} & [e^{k(D-z)} \hat{v} \\ & + e^{-k(D-z)} \hat{v}^*] \quad (48d) \end{aligned}$$

within the sea.

Magnitudes of electric and magnetic fields produced at the surface and sea bottom by a one meter high surface wave propagating in polar regions are shown in Figure 10 as functions of kD for a sea depth of one kilometer. Solid curves correspond to magnetic field magnitudes in gamma/m given on the left-hand coordinate scale, and dashed curves, to electric field magnitudes in $\mu V/m^2$ given on the right-hand coordinate.

For a fixed value of kD , field magnitudes are proportional to \sqrt{D} . As always, field magnitudes increase with decreasing wave number. Eventually, field magnitudes decrease with decreasing wave number as ocean wavelengths become comparable to electromagnetic wavelengths.

Magnitude and polarization of magnetic field profiles in polar regions are shown as functions of z/D in Figure 11 for $kD = 0.1$ and a sea depth of one kilometer. We observe that magnetic field profiles produced by ocean waves with wavelengths much greater than a sea depth are symmetrical. Magnitudes at the surface and sea bed are equal, and a relative minimum occurs at a depth of $D/2$. The field is circularly polarized in a right-handed sense at and above the surface, linearly polarized with a vertical alignment at a depth of $D/2$, and circularly polarized with a left-handed sense of rotation at and below the sea bed.

Fields induced in shallow seas in equatorial regions differ markedly from those in polar regions. Field magnitudes in equatorial regions not only are less than those in polar regions by a factor of $\cos \theta/2$, as before, but also decrease with wave number at small wave numbers, as shown by the solid curves in Figure 12, which displays magnetic field magnitudes at the ocean surface and bottom that are produced by one meter high surface waves propagating along magnetic meridians ($\theta=0$) in equatorial regions. Dashed curves in Figure 12 delineate magnitudes of the electrostatic component of the electric field at the ocean surface and bottom produced by one meter high surface waves propagating across magnetic meridians ($\theta=\pi/2$) in equatorial regions.

Profiles of magnetic field magnitude and polarization generated by a one meter high surface wave propagating along magnetic meridians in equatorial regions are shown in Figure 13a, which corresponds to an ocean depth of 1 km and $kD = 0.1$. We observe that profiles are no longer symmetrical, as in polar regions, and that a relative minimum occurs at a depth of $D/4$ rather than $D/2$. Elongation of polarization ellipses, however, retains a vertical bias.

Magnitude and polarization profiles of the electrostatic part of the field are shown as functions of z/D in Figure 13b. Profiles correspond to a one meter high surface wave propagating across magnetic meridians in equatorial regions and having a wavelength corresponding to $kD = 0.1$ in an ocean 1 km deep. We observe that magnitude of the field within the sea is effectively independent of depth and that its polarization is highly elongated with a vertical alignment. At the ocean floor, the field is linearly polarized in a vertical direction and so vanishes in suboceanic strata. Above the surface, however, the field is circularly polarized, and its magnitude is equal to the magnitude of the horizontal field component immediately below the surface.

At intermediate latitudes, field magnitudes are less than those in polar regions by the factor R given by Equation (35c), and the decrease in field magnitudes at small wave numbers lessens.

B. INTERNAL WAVES

For an ocean of depth D , we write the profile of the velocity potential for a progressive internal wave as

$$\psi_2 = \psi_d [\cosh k(z-d) - p_d \sinh k(z-d)] \quad (49a)$$

below the thermocline ($d \leq z \leq D$). The profile above the thermocline, ψ_1 , is expressed by Equation (36a). The vertical component of velocity vanishes at the ocean floor, so that

$$p_d = \tanh k(D-d) \quad . \quad (49b)$$

Continuity of pressure and the vertical component of velocity at the thermocline interface then gives the dispersion relation

$$\eta^2 = \frac{\Delta\rho/\rho}{\coth kd + \coth k(D-d)} \quad (49c)$$

where $\eta^2 = \omega^2/gk$ as before. Continuity of the vertical component of velocity alone at the thermocline interface gives the relation

$$-p_d \psi_d = \psi_o \sinh kd (1 - \eta^2 \coth kd) \quad (49d)$$

between values of respective profiles at the surface, ψ_o , and the thermocline interface, ψ_d . Finally, the kinematical relation gives the expression

$$i \left(\frac{\omega}{k} \right) \xi_d = p_d \psi_d \quad (49e)$$

for the thermocline displacement, ξ_d .

As before, electric and magnetic field profiles above the surface are expressed by Equations (25a) and (25b), and fields above the thermocline, by Equations (40a) and (40b). Below the thermocline, we express the profile of the electromagnetic potential as the sum of exponentials

$$\phi_{s2} = C_3 e^{-\alpha(D-z)} + C_4 e^{\alpha(D-z)} \quad (50a)$$

and corresponding electric and magnetic field profiles as

$$\begin{aligned} \vec{\epsilon}_{s2} = & ik \left\{ \phi_{s2} + \frac{\psi_d}{\sqrt{2} \cosh k(D-d)} \left[(\vec{B} \cdot \hat{v}) e^{k(D-z)} \right. \right. \\ & \left. \left. + (\vec{B} \cdot \hat{v}^*) e^{-k(D-z)} \right] \right\} \hat{n} \\ & - \frac{ik \psi_d}{\sqrt{2} \cosh k(D-d)} (\vec{B} \cdot \hat{n}) \left[e^{k(D-z)} \hat{v} + e^{-k(D-z)} \hat{v}^* \right] \quad (50b) \end{aligned}$$

and

$$\begin{aligned} \left(\frac{\omega}{k} \right) \vec{\beta}_{s2} = & \frac{ik}{\sqrt{2}} \left\{ C_4 \left(\frac{\alpha}{k} + 1 \right) e^{\alpha(D-z)} - C_3 \left(\frac{\alpha}{k} - 1 \right) e^{-\alpha(D-z)} \right. \\ & + \frac{\psi_d \sqrt{2} (\vec{B} \cdot \hat{v})}{\cosh k(D-d)} e^{k(D-z)} \left\{ \hat{v} + \frac{iK}{\sqrt{2}} \left\{ C_4 \left(1 - \frac{\alpha}{k} \right) e^{\alpha(D-z)} \right. \right. \\ & + C_3 \left(\frac{\alpha}{k} + 1 \right) e^{-\alpha(D-z)} \\ & \left. \left. + \frac{\psi_d \sqrt{2} (\vec{B} \cdot \hat{v})}{\cosh k(D-d)} e^{-k(D-z)} \right\} \hat{v}^* \right\} \quad (50c) \end{aligned}$$

We again represent suboceanic strata as a vacuum region of indefinite extent and so express electric and magnetic field profiles below the ocean as

$$\vec{\epsilon}_c = \left(\frac{\omega}{k}\right) (\hat{z} \cdot \vec{\beta}_c) \hat{n} \quad (50d)$$

and

$$\left(\frac{\omega}{k}\right) \vec{\beta}_c = \frac{ik}{\sqrt{2}} 2C_5 e^{-k(z-D)} \hat{n} \quad (50e)$$

Constants specifying the electromagnetic potential profile in each layer, obtained by requiring continuity of horizontal field vectors at each interface, are listed in the Appendix. Here, we express field profiles to first order in δ^2 .

By using Equation (49c), we express the square of the ratio of ocean wavelength to electromagnetic wavelength as

$$\frac{\delta^2}{2} = \frac{\mu_0 \sigma}{2k} \left[\frac{dg (\Delta\rho/\rho)}{kd (\coth kd + \coth k(D-d))} \right]^{1/2} \quad (51a)$$

so that

$$\frac{\delta^2}{2} < (4 \times 10^{-7}) \lambda [dg (\Delta\rho/\rho)(1 - d/D)]^{1/2} \quad (51b)$$

In both deep and shallow seas, then, internal wavelengths less than a few hundred kilometers are much smaller than corresponding electromagnetic wavelengths.*

* For internal wavelengths of the order of 100 km or greater, however, internal wave periods are comparable to tidal periods, so that Coriolis forces influence wave propagation and flow fields are no longer irrotational.

By neglecting η^2 compared to unity, as before, and using the first order expression for the ratio α/k , as given by Equation (30d), we express field profiles to first order in δ^2 as

$$\vec{\epsilon}_a = \left(\frac{\omega}{k}\right) (\hat{z} \cdot \vec{\beta}_a) \hat{n} \quad (52a)$$

and

$$\vec{\beta}_a = \frac{ik\xi_d \delta^2 \sinh kD}{2 \sinh k(D-d)} \left[\frac{kd e^{-kd}}{\sinh kd} - \frac{kD e^{-kD}}{\sinh kD} \right] e^{kz} (\vec{B} \cdot \hat{v}^*) \hat{v}^* \quad (52b)$$

above the surface ($z \leq 0$), as

$$\vec{\epsilon}_{s1} = \left(\frac{\omega}{k}\right) (\hat{z} \cdot \vec{\beta}_{s1}) \hat{n} - \frac{\omega \xi_d}{2 \sinh kd} (\vec{B} \cdot \hat{n}) \sqrt{2} (e^{-kz} \hat{v} + e^{kz} \hat{v}^*) \quad (52c)$$

and

$$\begin{aligned} \vec{\beta}_{s1} = & ik\xi_d \frac{\delta^2}{2} \left\{ \left[(\vec{B} \cdot \hat{v}^*) + (\vec{B} \cdot \hat{v}) \frac{kz e^{-kz}}{\sinh kz} \right] \left(\frac{\sinh kz}{\sinh kd} \right) \hat{v} \right. \\ & - \left[\left(\frac{\sinh kz}{\sinh kd} \right) (\vec{B} \cdot \hat{v}) - \frac{(\vec{B} \cdot \hat{v}^*) \sinh kD}{\sinh k(D-d)} \left(\frac{k(d-z) e^{-k(d-z)}}{\sinh kd} \right. \right. \\ & \left. \left. - \frac{k(D-z) e^{-k(D-z)}}{\sinh kD} \right) \right] \hat{v}^* \left. \right\} \quad (52d) \end{aligned}$$

above the thermocline ($0 \leq z \leq d$), and as

$$\begin{aligned} \vec{\epsilon}_{s2} = & \left(\frac{\omega}{k} \right) (\hat{z} \cdot \vec{\beta}_{s2}) \hat{n} + \frac{\omega \xi_d}{2 \sinh k(D-d)} (\vec{B} \cdot \hat{n}) \sqrt{2} \left[e^{k(D-z)} \hat{v} \right. \\ & \left. + e^{-k(D-z)} \hat{v}^* \right] \end{aligned} \quad (52e)$$

and

$$\begin{aligned} \vec{\beta}_{s2} = & -ik \xi_d \frac{\delta^2}{2} \left\{ \left[(\vec{B} \cdot \hat{v}) + (\vec{B} \cdot \hat{v}^*) \frac{k(D-z) e^{-k(D-z)}}{\sinh k(D-z)} \right] \left(\frac{\sinh k(D-z)}{\sinh k(D-d)} \right) \hat{v}^* \right. \\ & - \left[\frac{\sinh k(D-z)}{\sinh k(D-d)} (\vec{B} \cdot \hat{v}^*) \right. \\ & \left. \left. + \frac{(\vec{B} \cdot \hat{v})}{\sinh kd} \left(\frac{k(d-z) e^{k(d-z)} \sinh kD}{\sinh k(D-d)} + kz e^{-kz} \right) \right] \hat{v} \right\} \end{aligned} \quad (52f)$$

below the thermocline ($d \leq z \leq D$).

For purposes of illustration, we consider fields produced by a one meter high internal wave propagating along a 100 m deep thermocline in an ocean 1 km deep. We first consider fields induced in polar regions and then equatorial regions.

Magnitudes of electric and magnetic fields produced at the surface, bottom, and at the thermocline interface in polar regions are shown as functions of kD in Figure 14. Solid curves delineate magnetic field strengths per unit wave height in gamma/m corresponding to the left-hand coordinate scale, and dashed curves, electric field strengths per unit wave height in microvolts/m² corresponding to the

right-hand coordinate scale. For fixed values of kD and the depth ratio d/D , field magnitudes increase as the square root of thermocline depth. As for a deep ocean, field magnitudes at the surface decrease rapidly for internal wavelengths less than a thermocline depth. Furthermore, field magnitudes at the surface decrease rapidly for wavelengths greater than an ocean depth. Consequently, internal waves with wavelengths in the range, $d \leq \lambda \leq D$, alone produce an appreciable field at the surface.

Profiles of magnetic field magnitude and polarization produced in polar regions by internal waves having wavelengths much greater than an ocean depth, $kD = 0.5$, are shown in Figure 15. Except near the ocean floor, profiles are similar to those in a deep ocean, shown in Figure 4. An additional polarization reversal occurs near the ocean floor. For internal wavelengths much less than an ocean depth but yet much greater than a thermocline depth, we obtain profiles as shown in Figure 4. Finally, for internal wavelengths much less than a thermocline depth, and so also much less than an ocean depth, we obtain profiles as shown in Figure 5.

In equatorial regions, magnitudes of the transverse electric part of the electric field and the magnetic field are again less than values in polar regions by a factor of $\cos \theta/2$. Furthermore, polarization profiles and the dependence of field magnitudes at the thermocline interface on wave number change. Magnitudes of the magnetic field and the electrostatic part of the electric field in equatorial regions are shown as functions of kD in Figure 16.

Solid curves delineate magnetic field strengths produced at the surface, bottom, and at the thermocline interface per unit wave height in gamma/m, corresponding to the left-hand coordinate scale, by internal waves propagating along magnetic meridians ($\theta=0$). Dashed

curves represent magnitudes of the electrostatic part of the electric field produced per unit wave height immediately below the surface, $|\vec{E}_{o+}|/\xi_d$, immediately above and below the thermocline interface, $|\vec{E}_{d-}|/\xi_d$ and $|\vec{E}_{d+}|/\xi_d$ respectively, and immediately above the ocean floor $|\vec{E}_{o-}|/\xi_d$. Electric field magnitudes correspond to internal waves propagating across magnetic meridians ($\theta = \pi/2$) and are expressed in microvolts/m², corresponding to the right-hand coordinate scale. We note that the magnetic field strength at the thermocline interface now also decreases for small wave numbers.

Profiles of magnetic field magnitude and polarization in equatorial regions are shown in Figure 17a for $kD = 0.5$ and $\theta = 0$. We observe that polarization ellipses are predominantly aligned vertically as opposed to a predominant horizontal alignment in polar regions.

Finally, profiles of magnitude and polarization of the electrostatic part of the electric field are shown in Figure 17b. We observe that the field is linearly polarized with a vertical alignment at both the surface and ocean floor and that the electrostatic field vanishes above and below the sea.

V. CONCLUSION

To conclude, we summarize salient features of the electromagnetic field induced by progressive ocean waves and mark features germane to spectral measurements. First, the electromagnetic field is the sum of a transverse-electric type field and an electrostatic type field.

The electrostatic part of the field is polarized in a vertical plane containing the direction of wave propagation. Polarization of the field is independent of latitude. At the ocean floor, polarization is linear with a vertical alignment, for both surface and internal waves, so that the electrostatic field vanishes in suboceanic strata. Within the sea, polarization of the electrostatic field produced by surface waves is elliptical with a vertical major axis and a left-handed sense of rotation. Polarization ellipses are highly elongated for wavelengths of surface waves that are much greater than an ocean depth and are nearly circular for wavelengths much less than an ocean depth. Above the surface, polarization is circular with a right-handed sense of rotation.

Polarization of the electrostatic field produced by internal waves, however, is linear with a vertical alignment at the surface, so that the electrostatic part of the field vanishes above the surface.*

* A vertically aligned linear polarization at the surface results because surface displacements produced by internal waves are negligibly small.

Within the sea, polarization is elliptical with a vertical major axis and a right-handed sense of rotation above the thermocline and a left-handed sense of rotation below the thermocline. Polarization ellipses above the thermocline are highly elongated for wavelengths of internal waves that are much greater than a thermocline depth and are nearly circular (except near the surface) for wavelengths much greater than a thermocline depth. Below the thermocline, polarization ellipses are highly elongated for wavelengths much less than an ocean depth and are nearly circular (except near the ocean floor) for wavelengths much less than an ocean depth.

Magnitude of the electrostatic part of the field is proportional to the horizontal component of the Earth's magnetic field that is transverse to the direction of wave propagation and so vanishes in polar regions and for waves propagating along magnetic meridians. Magnitudes are greatest in equatorial regions for waves propagating across magnetic meridians. Maximum magnitudes of the electrostatic field immediately below the surface produced per unit surface wave height are a few microvolts/m² for wavelengths much greater than an ocean depth and increase as the square root of wave number for wavelengths much less than an ocean depth. Electrostatic field strength and current density at the surface are the only surface quantities that increase with wave number.

Maximum electrostatic field strengths produced immediately below the surface per unit internal wave height are a few tenths of microvolts/m² for wavelengths much greater than a thermocline depth and decrease rapidly for wavelengths much less than a thermocline depth. Electrostatic field strengths at the thermocline interface, however, increase as the square root of wave number.

The magnetic field of the transverse electric part of the field is polarized in a vertical plane containing the direction of wave propagation, and the electric field, by definition, is linearly polarized in the horizontal direction transverse to the direction of wave propagation. Within the sea, polarization of the magnetic field produced by both surface and internal waves varies markedly with both depth and latitude. At and above the surface, however, polarization is always circular with a right-handed sense of rotation, whatever the type of wave motion or latitude.

Magnitude of the magnetic field is proportional to the product of wave height* and phase speed of ocean waves, provided wavelengths are smaller than electromagnetic wavelengths and much greater than wave heights. Magnitude of the transverse electric field is the product of phase speed and the vertical component of the induced magnetic field and thus is proportional to the product of wave height and the square of phase speed. As a result, field magnitudes per unit wave height increase with decreasing wave number and attain maximum values at small wave numbers — much as do phase speeds. Magnitudes are also greater in polar regions than equatorial regions because the Earth's field is stronger in polar regions.

In polar regions, magnetic and electric field strengths at the ocean surface and bottom produced by surface waves are reinforced by surface and bottom reflections for wavelengths greater than an ocean depth. Similarly, field strengths at a thermocline interface produced by internal waves are reinforced by reflections, but field strengths at the surface and bottom are reduced by interfering reflections at wavelengths

* Thermocline displacement is the wave height of an internal wave.

greater than an ocean depth. Surface waves produce maximum magnetic and electric field magnitudes per unit wave height of the order of 10 gamma/m and 1 microvolt/m², respectively, at the surface in polar regions. Maximum field magnitudes per unit wave height produced at the surface by internal waves are of the order of 0.1 gamma/m and 10⁻⁴ microvolts/m² in polar regions.

In equatorial regions, however, surface and bottom reflections interfere and so reduce magnetic and electric field strengths at the ocean surface and bottom produced by surface waves with wavelengths much greater than an ocean depth, as well as field strengths at a thermocline interface produced by internal waves. Maximum field strengths in equatorial regions are about one half those in polar regions, for waves propagating along magnetic meridians. The transverse electric part of the field vanishes for waves propagating across magnetic meridians in equatorial regions.

For purposes of spectral measurements, measurement of the induced magnetic field at or above the surface is most appropriate. Because electric field strengths are small, electrode separations of the order of tens of meters are required, which complicates interpretation of spectral measurements. Magnetic field measurements, however, are effectively point measurements, so that spectral features of the induced magnetic field are simply related to those of ocean waves. The power spectrum of the induced magnetic field is simply the product of the ocean wave power spectrum and the squared modulus of a transfer function, which is the magnetic field profile induced per unit wave height by a progressive wave. Consequently, dependence of the magnetic field profile induced per unit wave height at or above the surface on wave number is the feature of the electromagnetic field induced by a progressive ocean wave that is germane to spectral measurement.

In this regard, we note that magnetic field spectra are softer than ocean wave spectra because induced fields are greater at small wave numbers. Furthermore, spectra soften with increasing altitude, as the exponential decrease in field magnitudes with altitude is lesser at smaller wave numbers. We defer detailed description of spectral features, however, to a subsequent report.

FIGURE CAPTIONS

Figure 1. Magnitudes of electric and magnetic fields produced at the surface of a deep ocean by a one meter high surface wave propagating in polar regions shown as functions of wave number k along the lower abscissa and as functions of reciprocal wavelength, $1/\lambda$, along the upper abscissa. The solid curve delineates magnetic field strength per unit wave height in gamma/m and corresponds to the left-hand coordinate scale. The dashed curve delineates electric field strength per unit wave height in microvolts/m² and corresponds to the right-hand coordinate scale. Straight dashed lines are asymptotes for large and small wave numbers.

Figure 2. Profile of magnetic field magnitude and polarization produced in a deep ocean by a one meter high surface wave propagating in polar regions with a wavelength of 10 m corresponding to a frequency of about 0.4 Hz. Altitude and depth are measured in units of an ocean wavelength.

Figure 3. Magnitudes of electric and magnetic fields produced at the surface and at a 100 meter deep thermocline by a one meter high internal wave propagating in a deep ocean in polar regions shown as functions of dimensionless wave number kd along the lower abscissa and as functions of d/λ along the upper abscissa, where d denotes thermocline depth. Solid curves delineate magnetic field strengths per unit wave height in gamma/m and correspond to the left-hand coordinate

scale. Dashed curves delineate electric field strengths per unit wave height in microvolts/ m^2 and correspond to the right-hand coordinate scale.

Figure 4. Profile of magnetic field magnitude and polarization produced in a deep ocean containing a sharp thermocline at a depth of 100 meters by a one meter high internal wave propagating in polar regions and having a wavelength much greater than a thermocline depth, $kd = 0.1$. Altitude and depth are measured in units of a thermocline depth, d .

Figure 5. Profile of magnetic field magnitude and polarization produced in a deep ocean containing a sharp thermocline at a depth of 100 meters by a one meter high internal wave propagating in polar regions and having a wavelength much less than a thermocline depth, $kd = 4$. Altitude and depth are measured in units of a thermocline depth, d .

Figure 6. Magnitudes of the magnetic field and the electrostatic part of the electric field produced at the surface and at a 100 meter deep thermocline by a one meter high internal wave propagating in a deep ocean in equatorial regions shown as functions of kd along the lower abscissa and as functions of d/λ along the upper abscissa. Magnetic field magnitudes correspond to internal wave propagation along magnetic meridians, and electric field magnitudes, to propagation across magnetic meridians. Solid curves delineate magnetic field strengths per unit wave height in gamma/ m and correspond to the left-hand coordinate scale. Dashed curves delineate electric field strengths per unit wave height in microvolts/ m^2 and correspond to the right-hand coordinate scale.

Figure 7a. Profile of magnetic field magnitude and polarization produced in a deep ocean containing a sharp thermocline at a depth of 100 meters by a one meter high internal wave propagating along magnetic meridians in equatorial regions and having a wavelength much greater than a thermocline depth, $kd = 0.1$. Altitude and depth are measured in units of a thermocline depth, d .

Figure 7b. Profile of magnitude and polarization of the electrostatic part of the electric field produced in a deep ocean containing a sharp thermocline at a depth of 100 meters by a one meter high internal wave propagating across magnetic meridians in equatorial regions and having a wavelength much greater than a thermocline depth, $kd = 0.1$. Altitude and depth are measured in units of a thermocline depth, d .

Figure 8a. Profile of magnetic field magnitude and polarization produced in a deep ocean containing a sharp thermocline at a depth of 100 meters by a one meter high internal wave propagating along magnetic meridians in equatorial regions and having a wavelength much less than a thermocline depth, $kd = 4$. Altitude and depth are measured in units of a thermocline depth, d .

Figure 8b. Profile of magnitude and polarization of the electrostatic part of the electric field produced in a deep ocean containing a sharp thermocline at a depth of 100 meters by a one meter high internal wave propagating across magnetic meridians in equatorial regions and having a wavelength much less than a thermocline, $kd = 4$. Altitude and depth are measured in units of a thermocline depth, d .

Figure 9. Square of the ratio of wavelength of a surface wave on an ocean of depth D to wavelength of an electromagnetic wave, $\delta^2/2$, shown as a function of kD on the lower abscissa and as a function of D/λ on the upper abscissa for ocean depths of 10, 1, 0.5, and 0.1 kilometers. Straight dashed lines are asymptotes for large and small values of kD .

Figure 10. Magnitudes of electric and magnetic fields produced at the surface and bottom of an ocean 1 km in depth by a one meter high surface wave propagating in polar regions shown as functions of kD along the lower abscissa and as functions of D/λ along the upper abscissa, where D denotes ocean depth. Solid curves delineate magnetic field strengths per unit wave height in gamma/m and correspond to the left-hand coordinate scale. Dashed curves delineate electric field strengths per unit wave height in microvolts/m² and correspond to the right-hand coordinate scale.

Figure 11. Profile of magnetic field magnitude and polarization produced in an ocean 1 km deep by a one meter high surface wave propagating in polar regions and having a wavelength much greater than an ocean depth, $kD = 0.1$. Altitude and depth are measured in units of an ocean depth, D .

Figure 12. Magnitudes of the magnetic field and the electrostatic part of the electric field produced at the surface and bottom of an ocean 1 km in depth by a one meter high surface wave propagating in equatorial regions shown as functions of kD along the lower abscissa and as functions of D/λ along the upper abscissa. Magnetic field magnitudes correspond to surface wave propagation along magnetic meridians, and electric field magnitudes, to propagation across magnetic meridians.

Solid curves delineate magnetic field strengths per unit wave height in gamma/m and correspond to the left-hand coordinate scale. Dashed curves delineate electric field strengths per unit wave height in microvolts/m² and correspond to the right-hand coordinate scale.

Figure 13a. Profile of magnetic field magnitude and polarization produced in an ocean 1 km deep by a one meter high surface wave propagating along magnetic meridians in equatorial regions and having a wavelength much greater than an ocean depth, $kD = 0.1$. Altitude and depth are measured in units of an ocean depth, D .

Figure 13b. Profile of magnitude and polarization of the electrostatic part of the electric field produced in an ocean 1 km deep by a one meter high surface wave propagating across magnetic meridians in equatorial regions and having a wavelength much greater than an ocean depth, $kD = 0.1$. Altitude and depth are measured in units of an ocean depth, D .

Figure 14. Magnitudes of electric and magnetic fields produced at the surface, bottom, and at a 100 meter deep thermocline in an ocean 1 km deep by a one meter high internal wave propagating in polar regions shown as functions of kD along the lower abscissa and as functions of D/λ along the upper abscissa, where D denotes ocean depth. Solid curves delineate magnetic field strengths per unit wave height in gamma/m and correspond to the left-hand coordinate scale. Dashed curves delineate electric field strengths per unit wave height in microvolts/m² and correspond to the right-hand coordinate scale.

Figure 15. Profile of magnetic field magnitude and polarization produced in an ocean 1 km deep containing a sharp thermocline at a depth of 100 m by a one meter high internal wave propagating in polar regions and having a wavelength much greater than an ocean depth, $kD = 0.5$. Altitude and depth are measured in units of a thermocline depth, d .

Figure 16. Magnitudes of the magnetic field and electrostatic part of the electric field produced at the surface, bottom, and at a 100 meter deep thermocline in an ocean 1 km deep by a one meter high internal wave propagating in equatorial regions shown as functions of kD along the lower abscissa and as functions of D/λ along the upper abscissa. Magnetic field magnitudes correspond to internal wave propagation along magnetic meridians, and electric field magnitudes, to propagation across magnetic meridians. Solid curves delineate magnetic field strengths per unit wave height in gamma/m and correspond to the left-hand coordinate scale. Dashed curves delineate electric field strengths per unit wave height in microvolts/m² and correspond to the right-hand coordinate scale.

Figure 17a. Profile of magnetic field magnitude and polarization produced in an ocean 1 km deep containing a sharp thermocline at a depth of 100 m by a one meter high internal wave propagating along magnetic meridians in equatorial regions and having a wavelength much greater than an ocean depth, $kD = 0.5$. Altitude and depth are measured in units of a thermocline depth, d .

Figure 17b. Profile of magnitude and polarization of the electrostatic part of the electric field produced in an ocean 1 km deep containing a sharp thermocline at a depth of 100 m by a one meter high internal

wave propagating across magnetic meridians in equatorial regions and having a wavelength much greater than an ocean depth, $kD = 0.5$. Altitude and depth are measured in units of a thermocline depth, d .

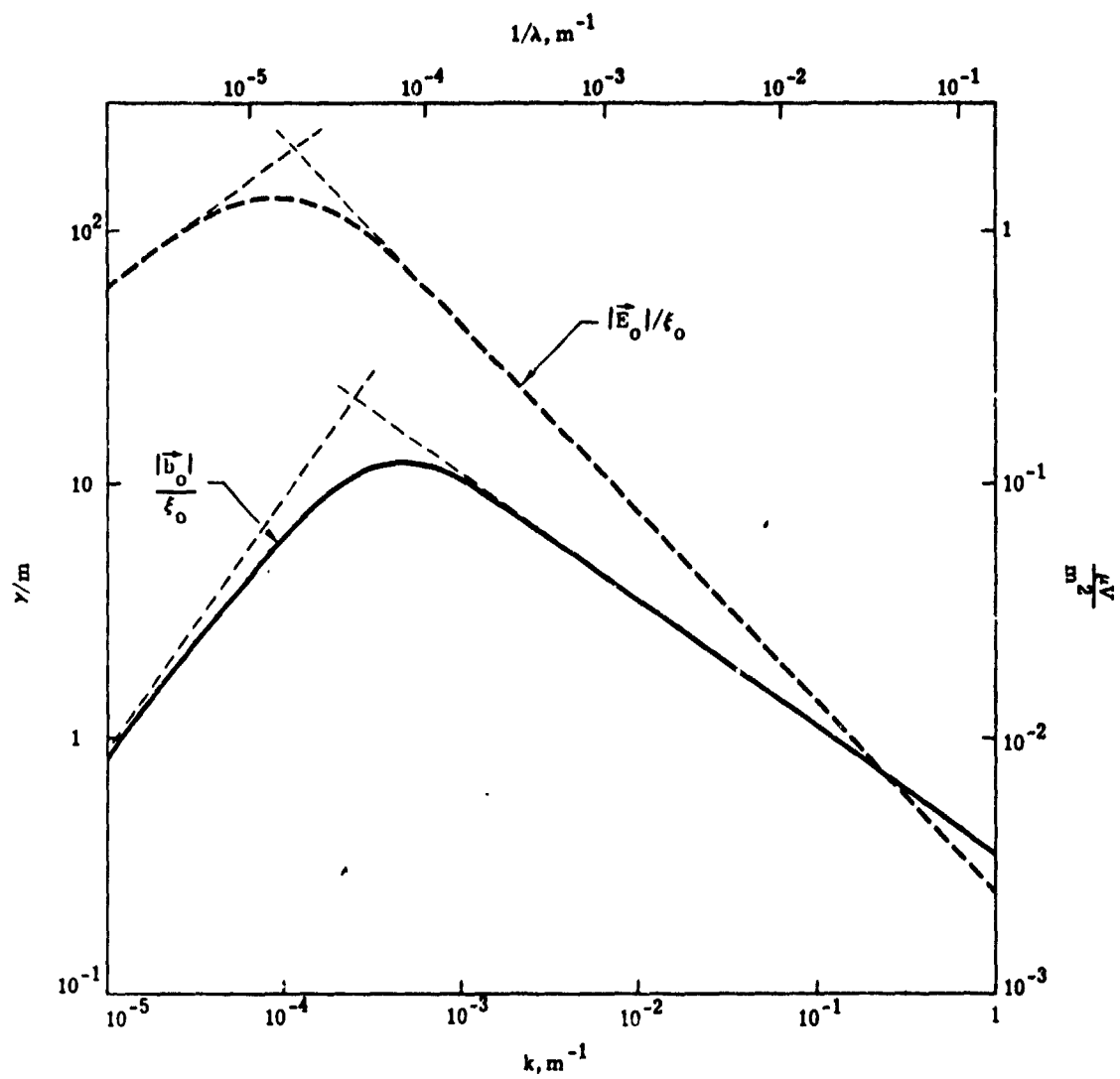


Figure 1

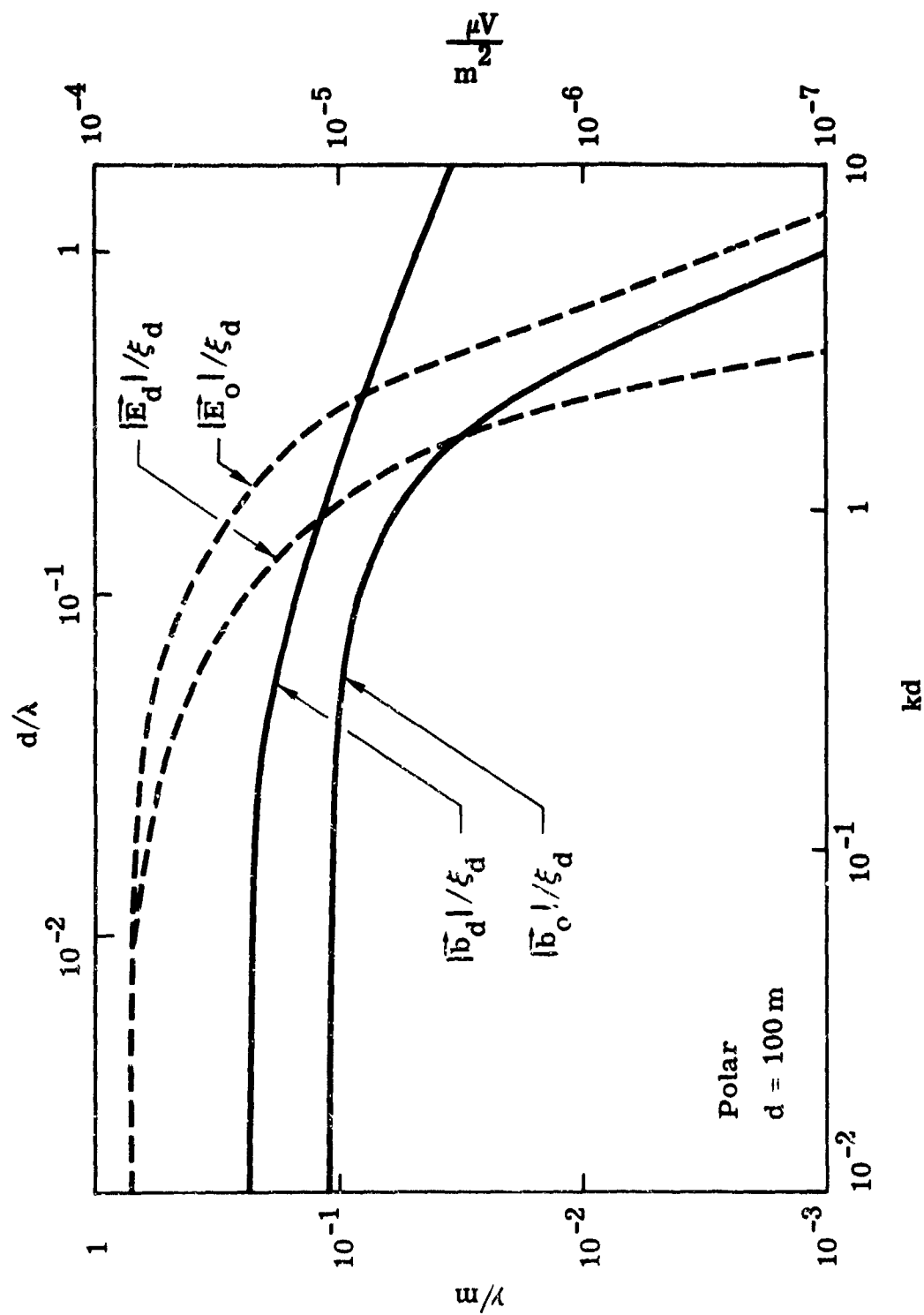


Figure 3

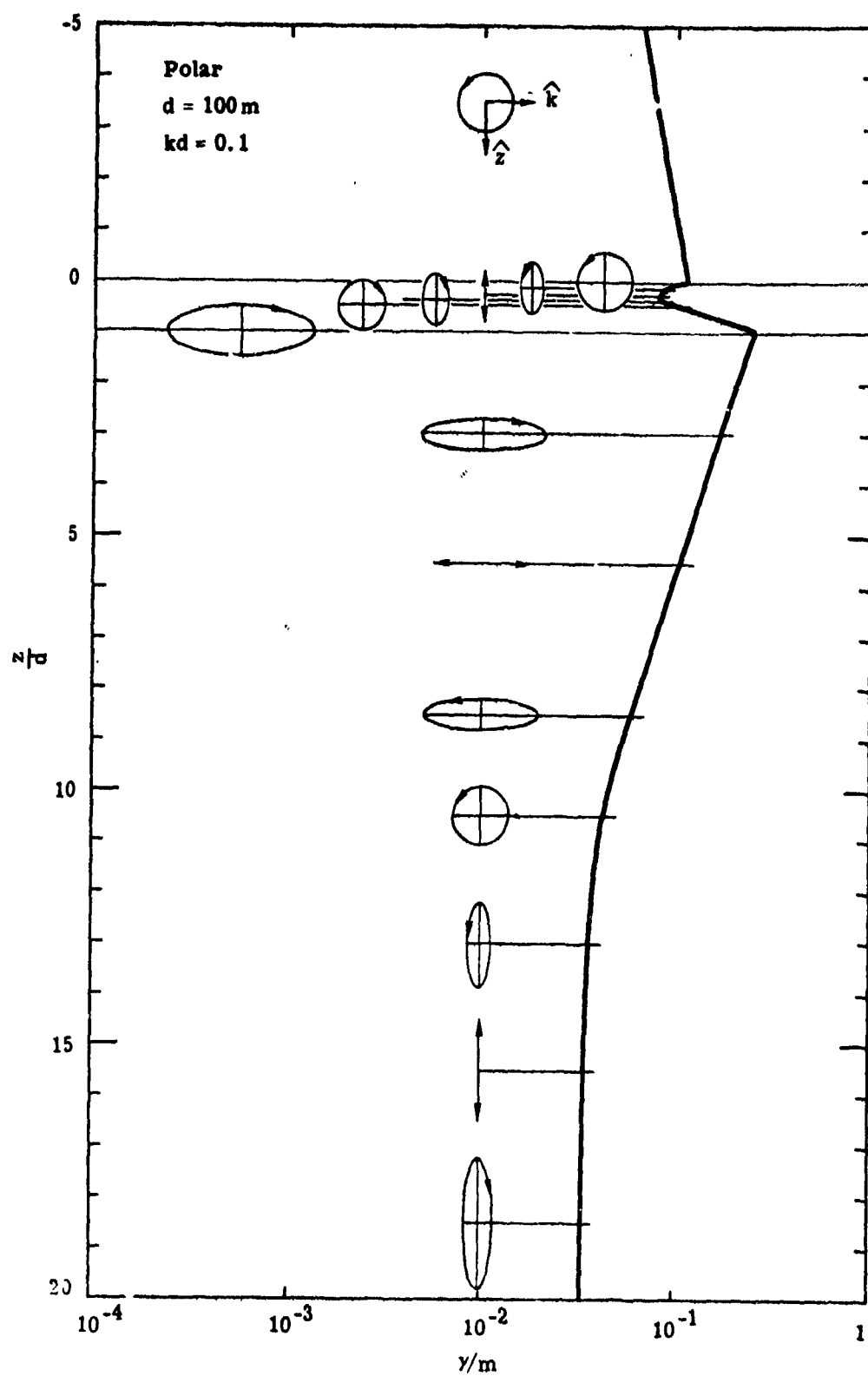


Figure 4

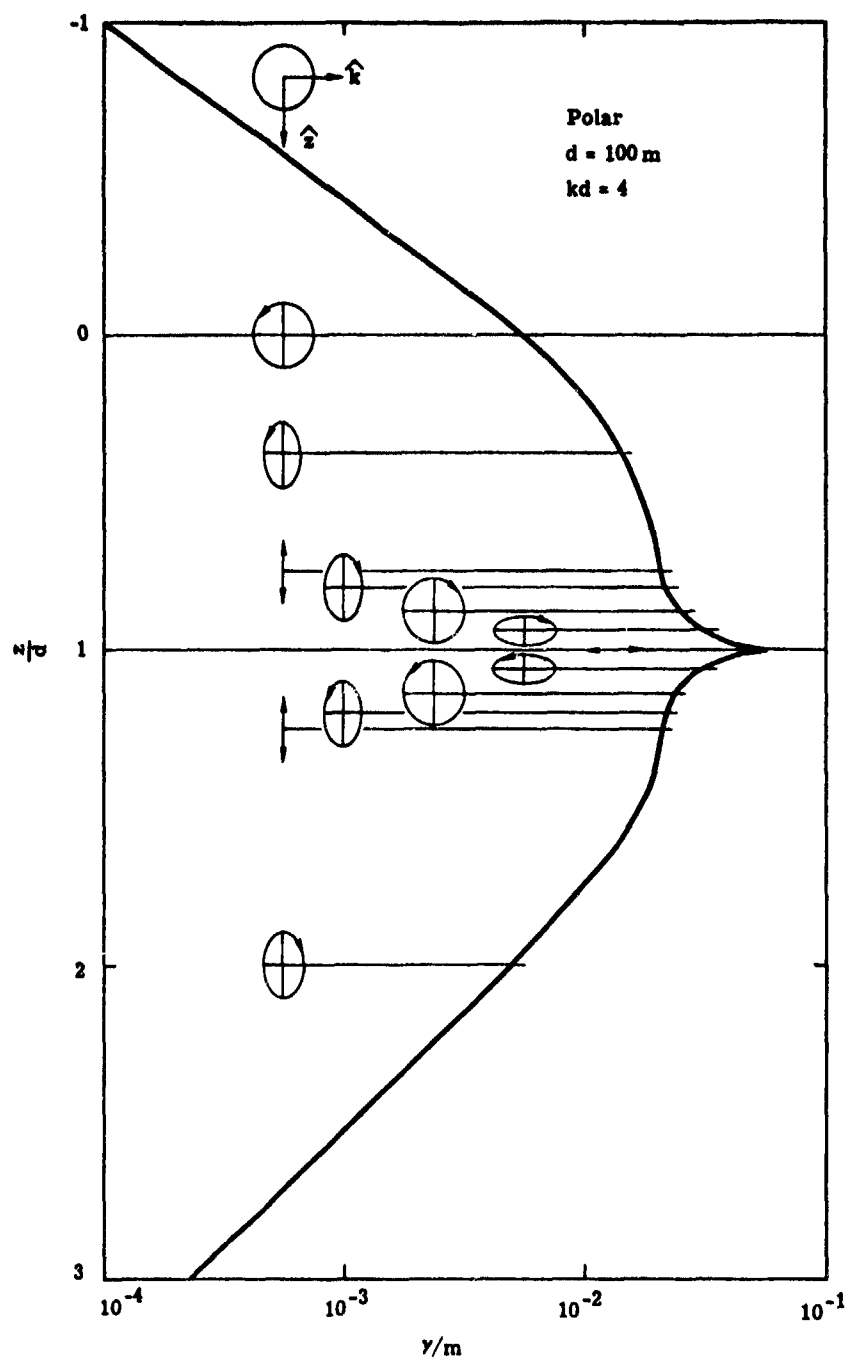


Figure 5

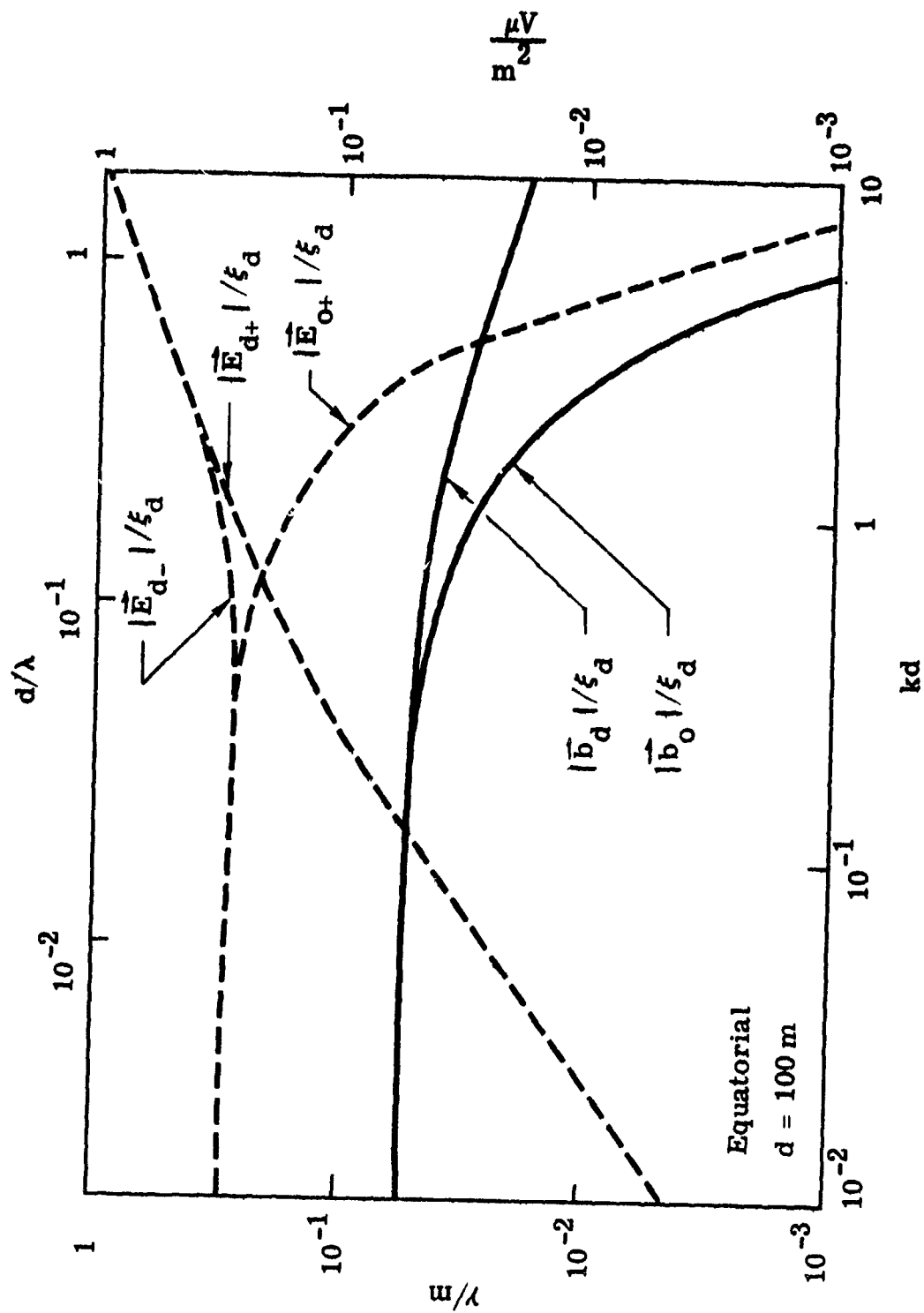


Figure 6

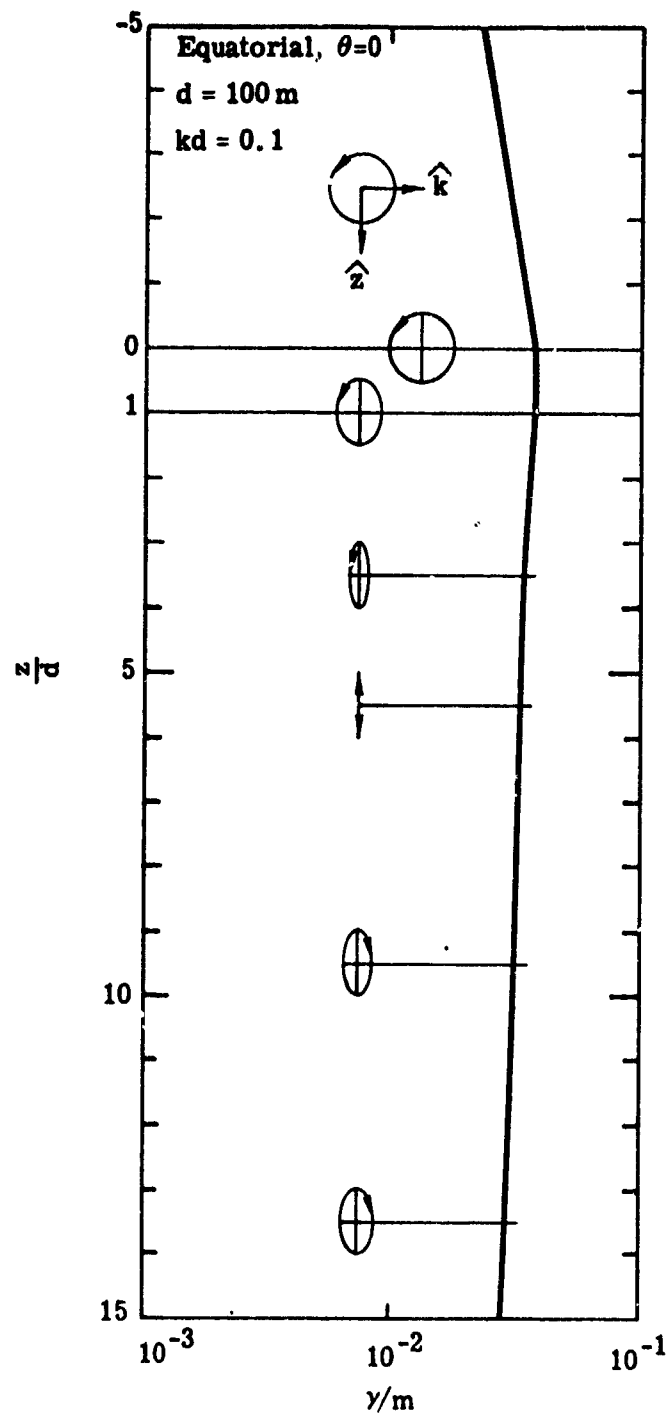


Figure 7a

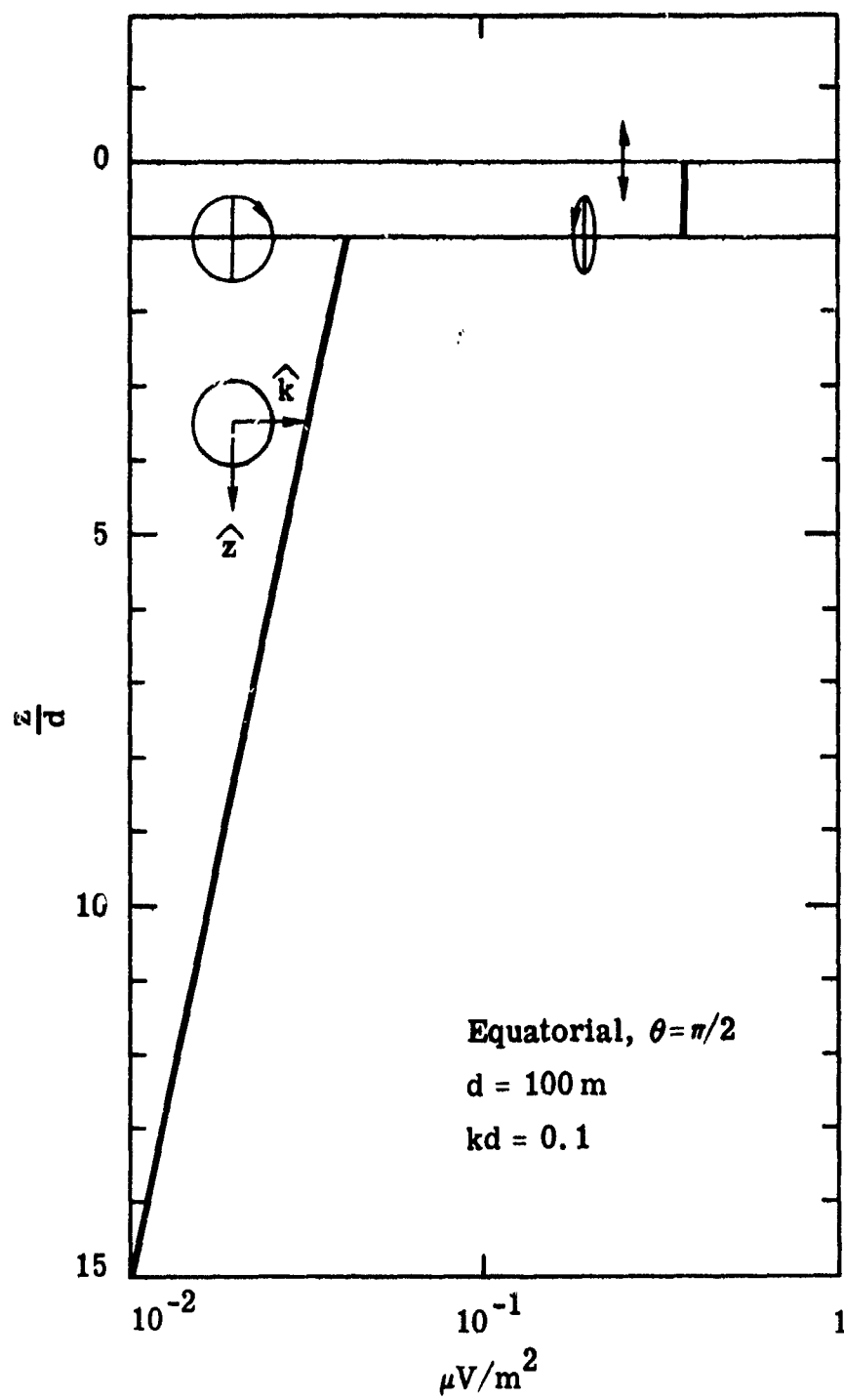


Figure 7b

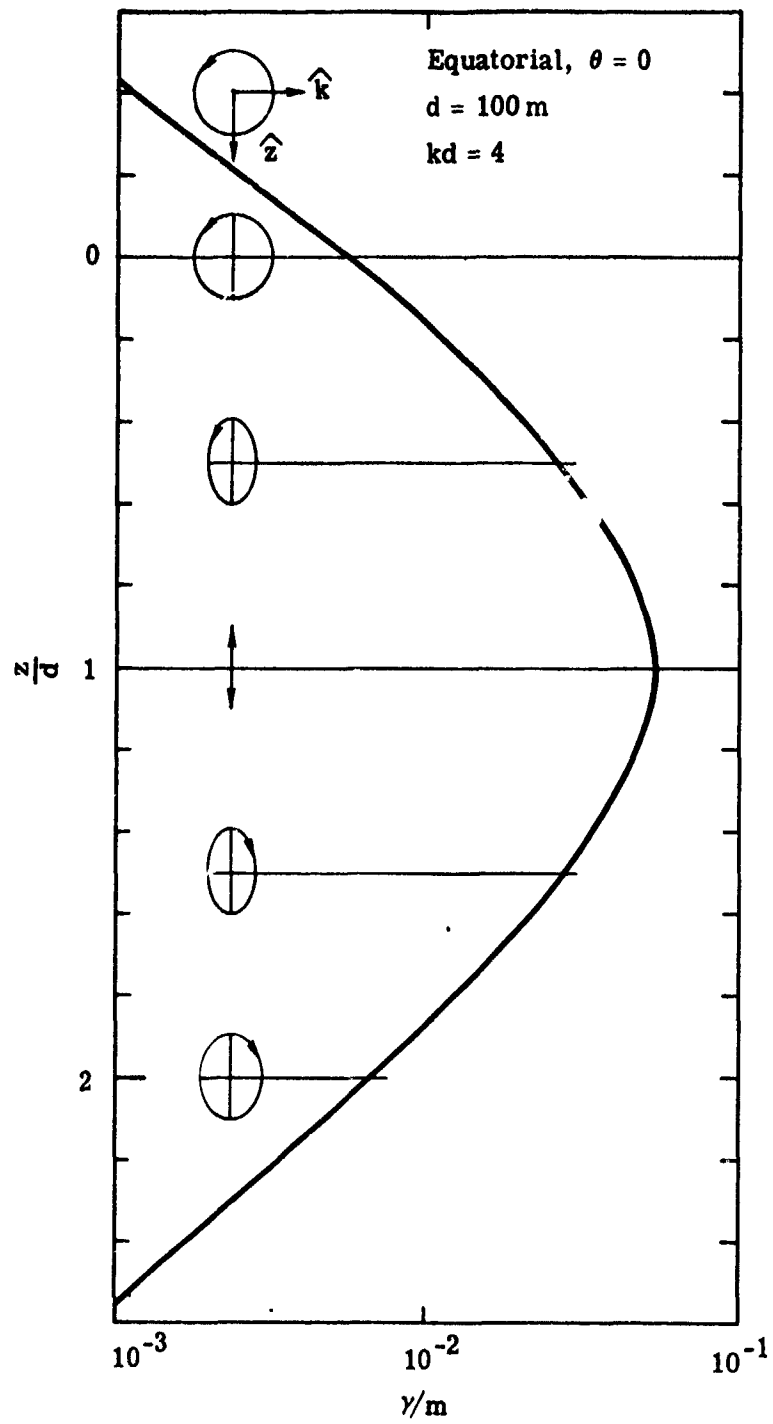


Figure 8a

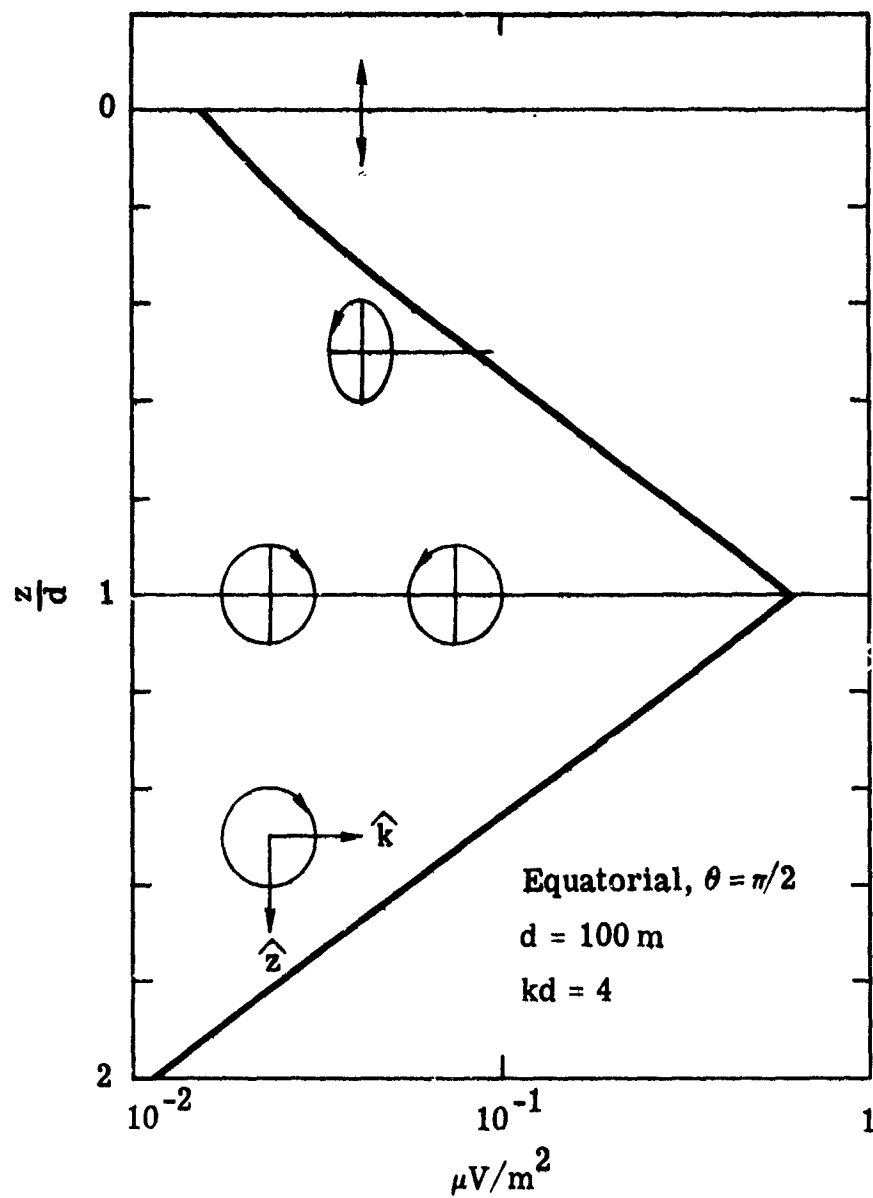


Figure 8b

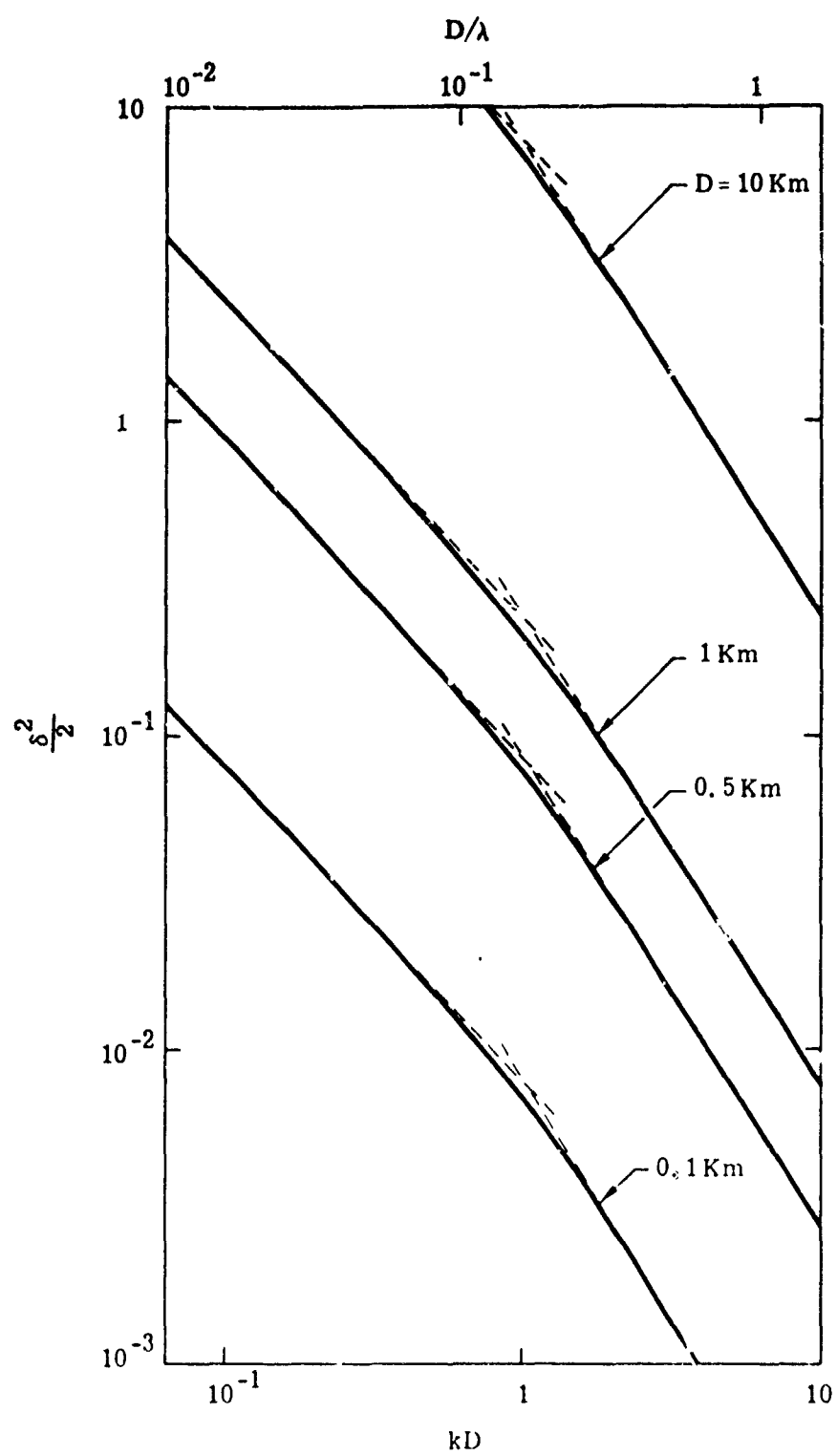


Figure 9

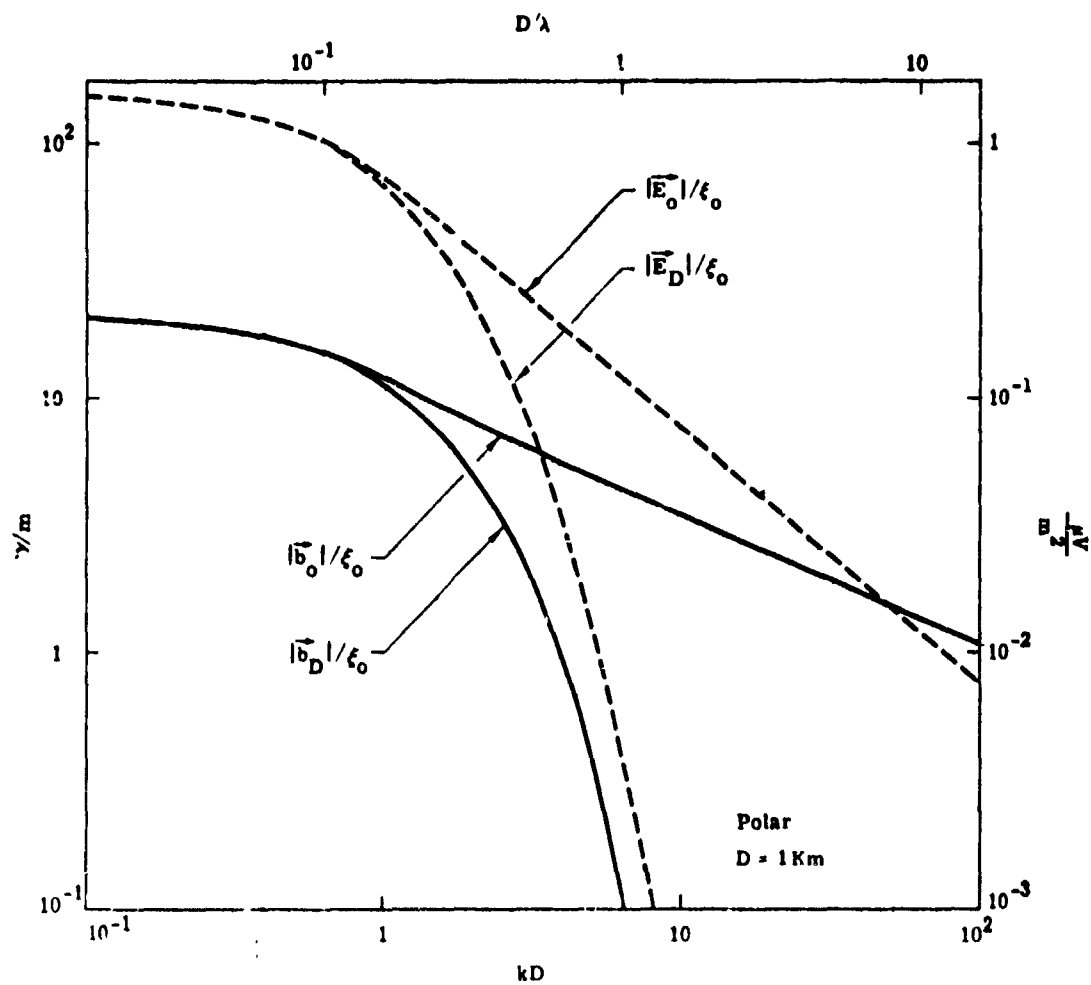


Figure 10

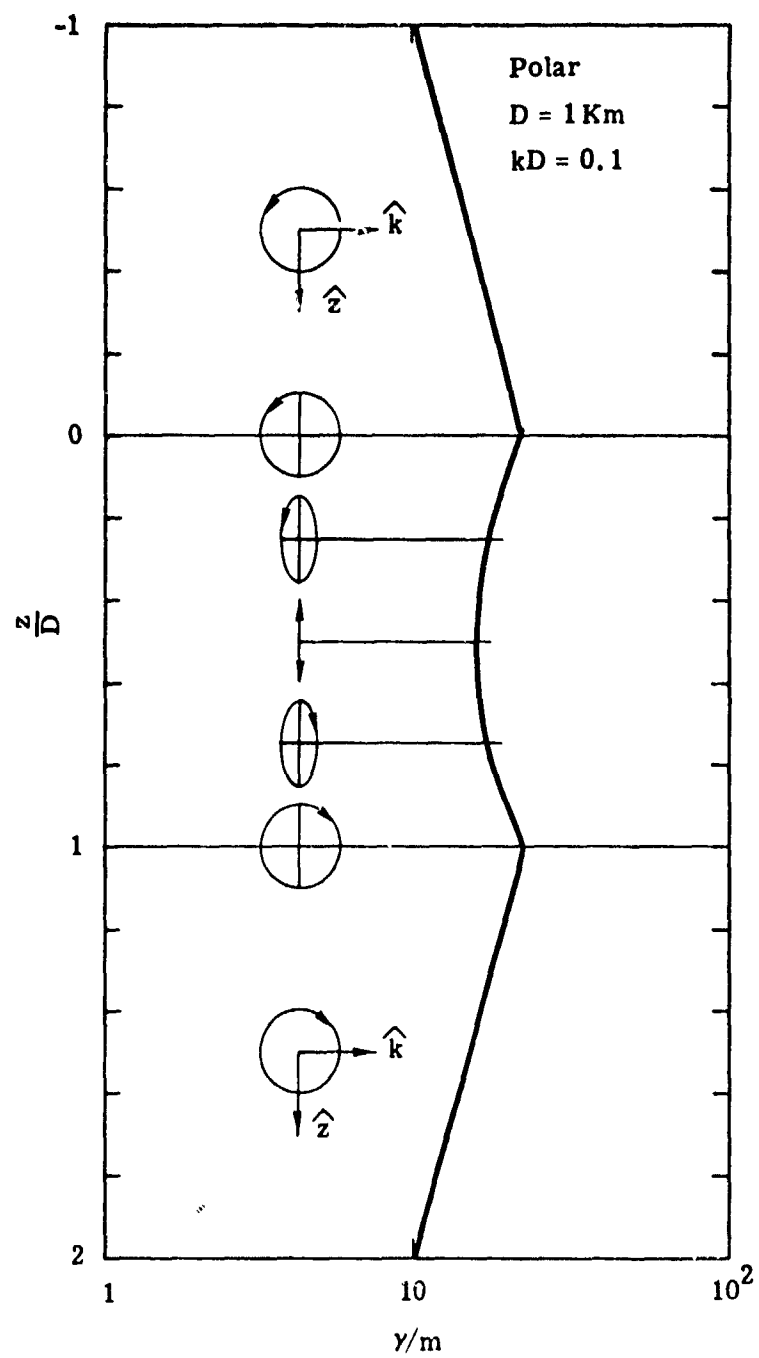


Figure 11

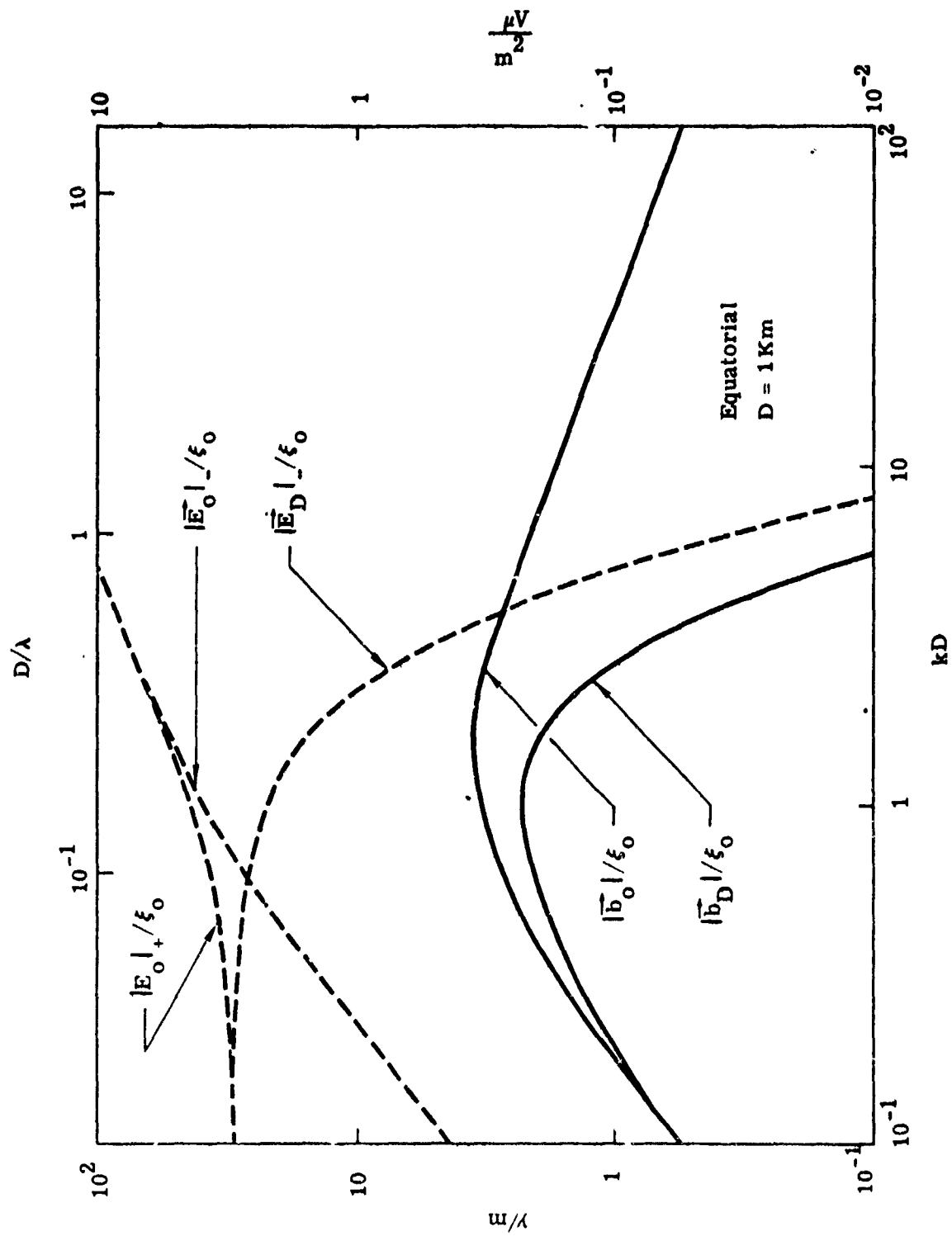


Figure 12

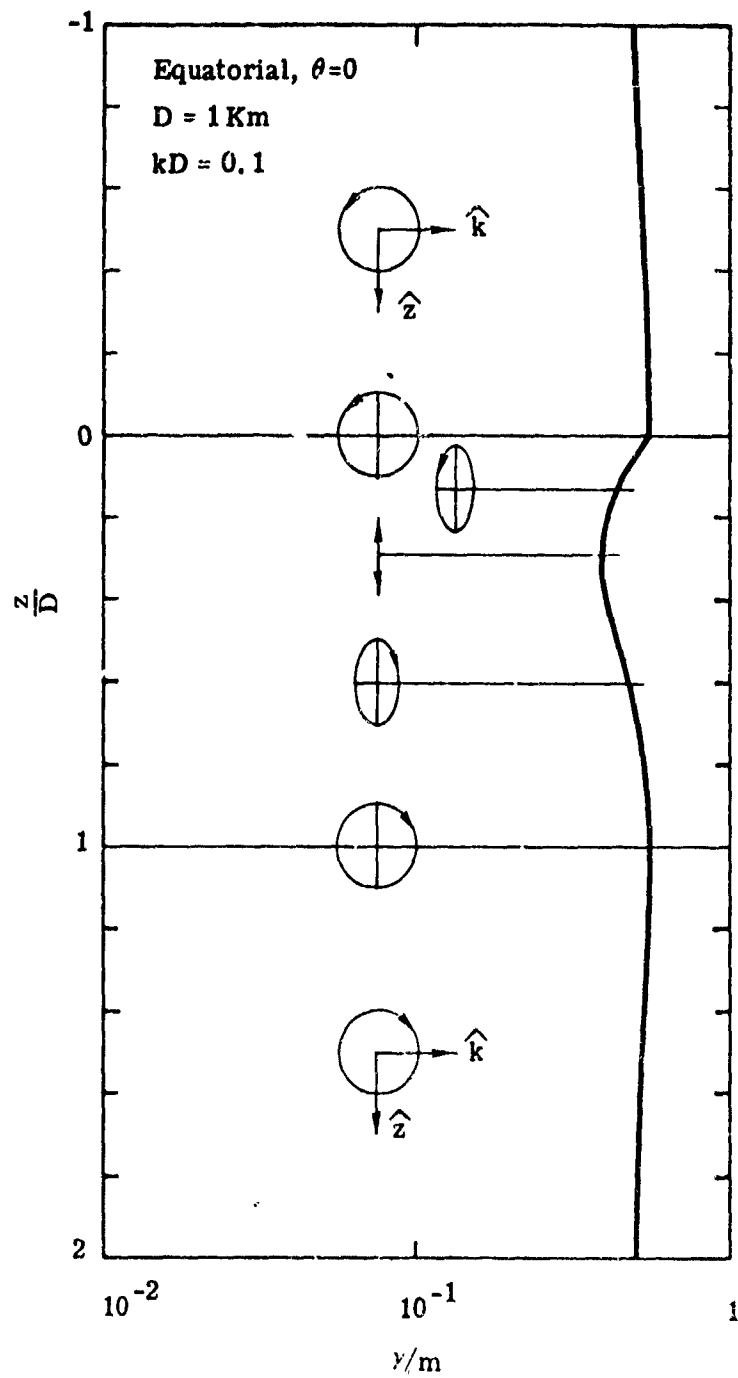


Figure 13a

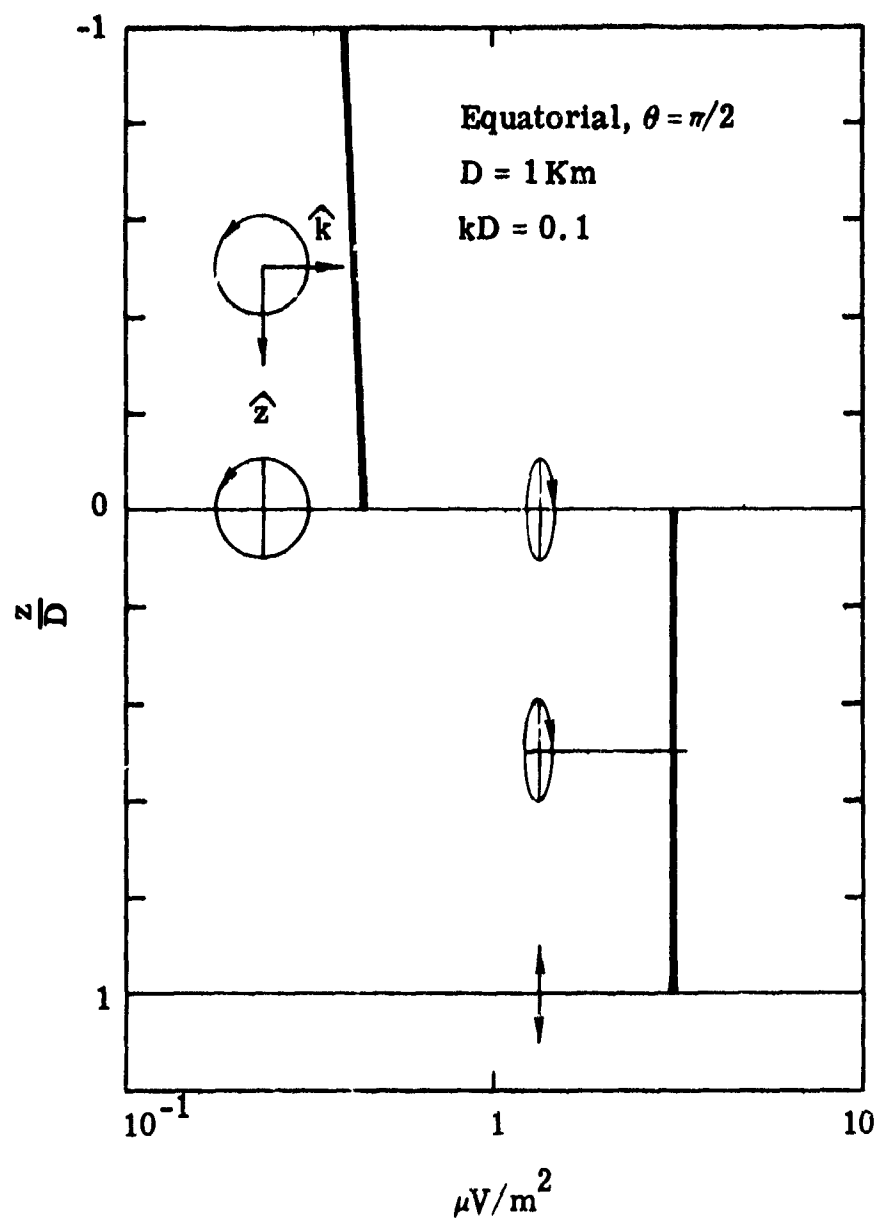


Figure 13b

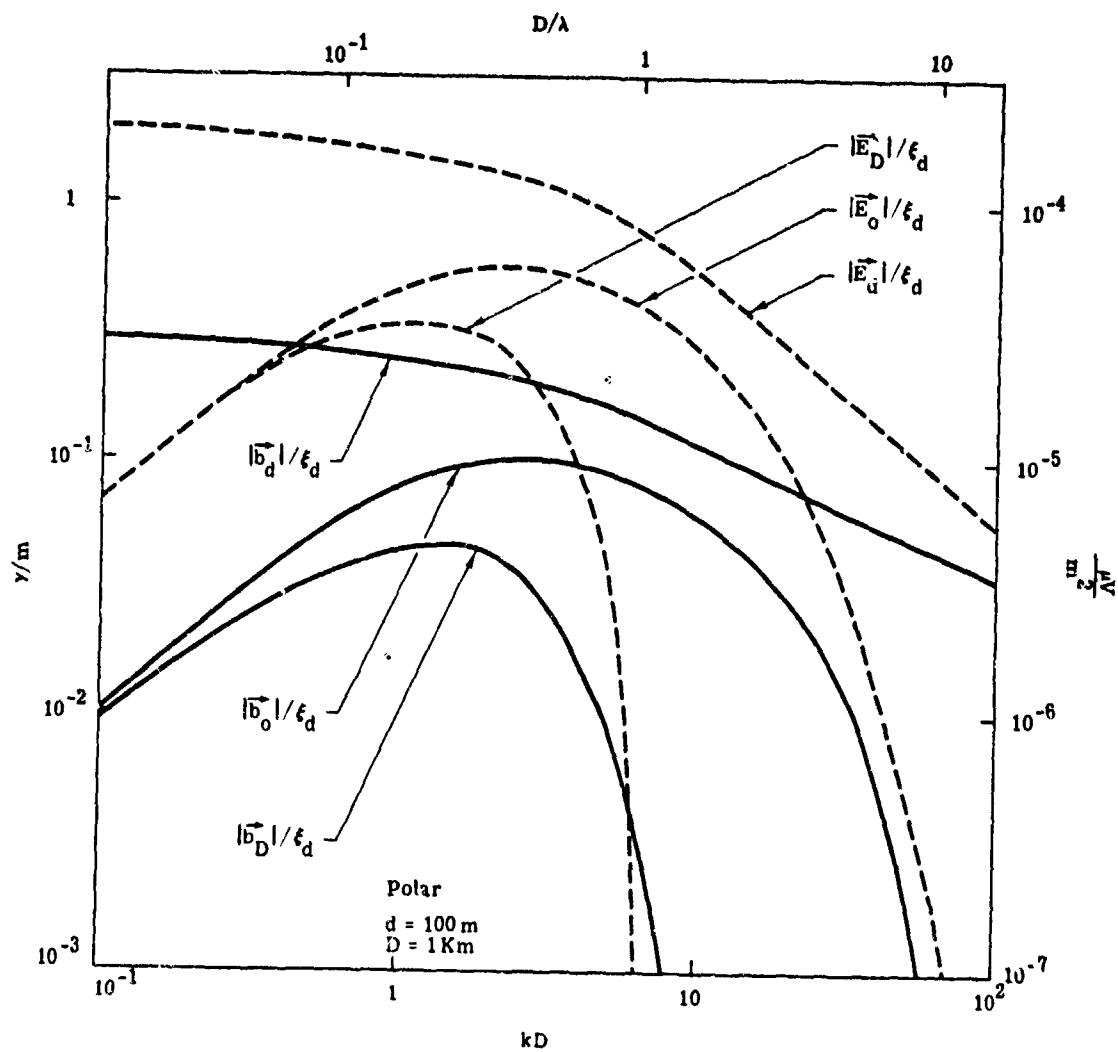


Figure 14

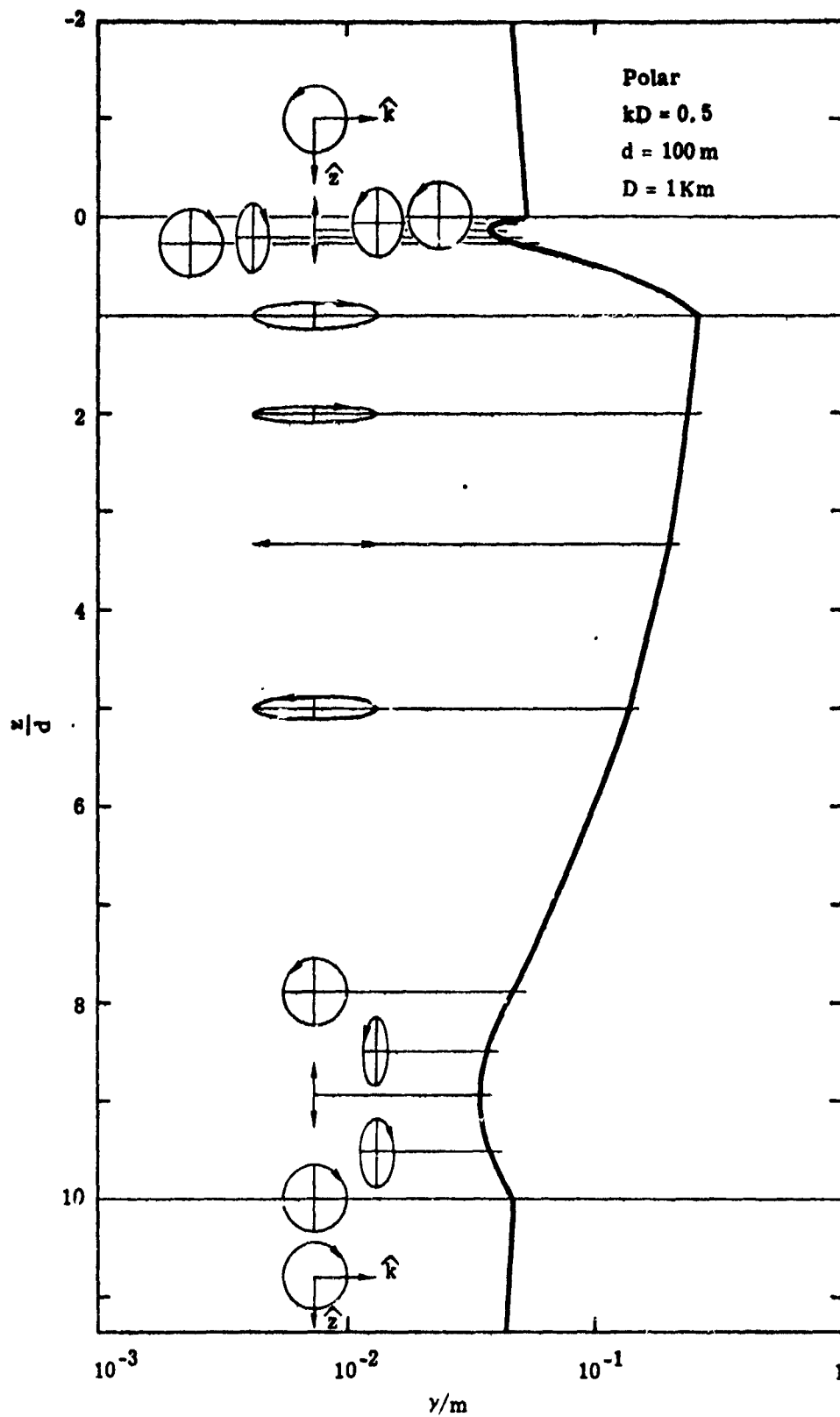


Figure 15

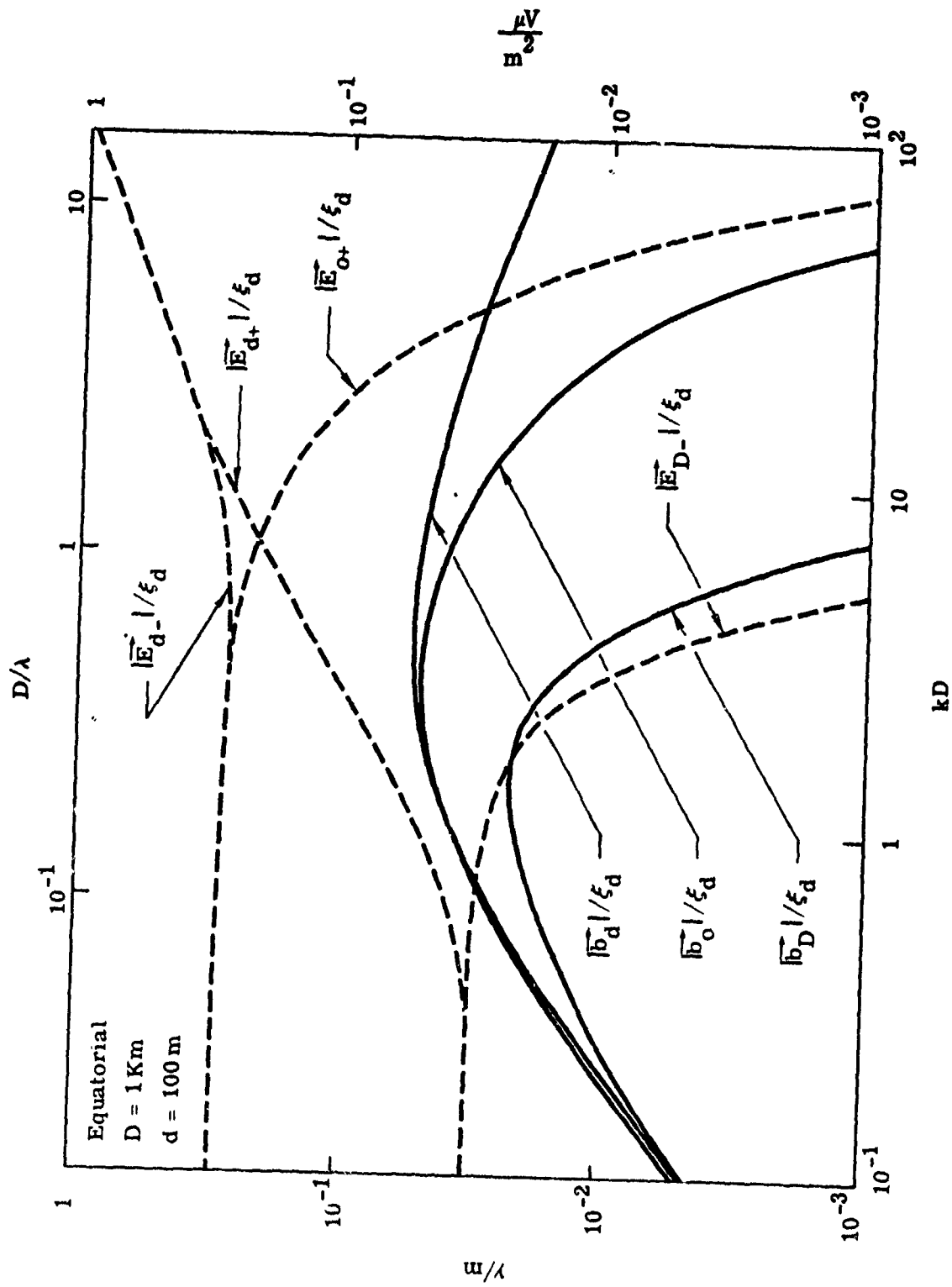


Figure 16

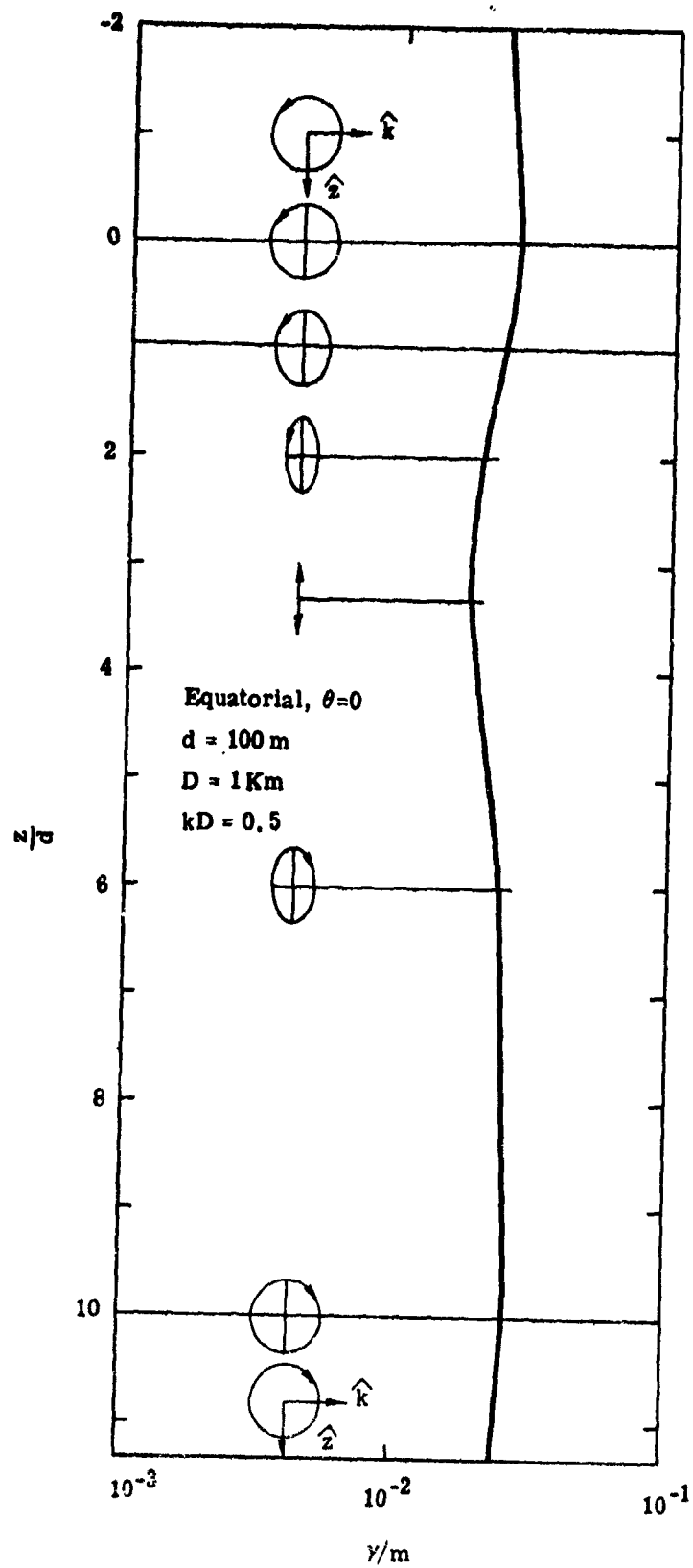


Figure 17a

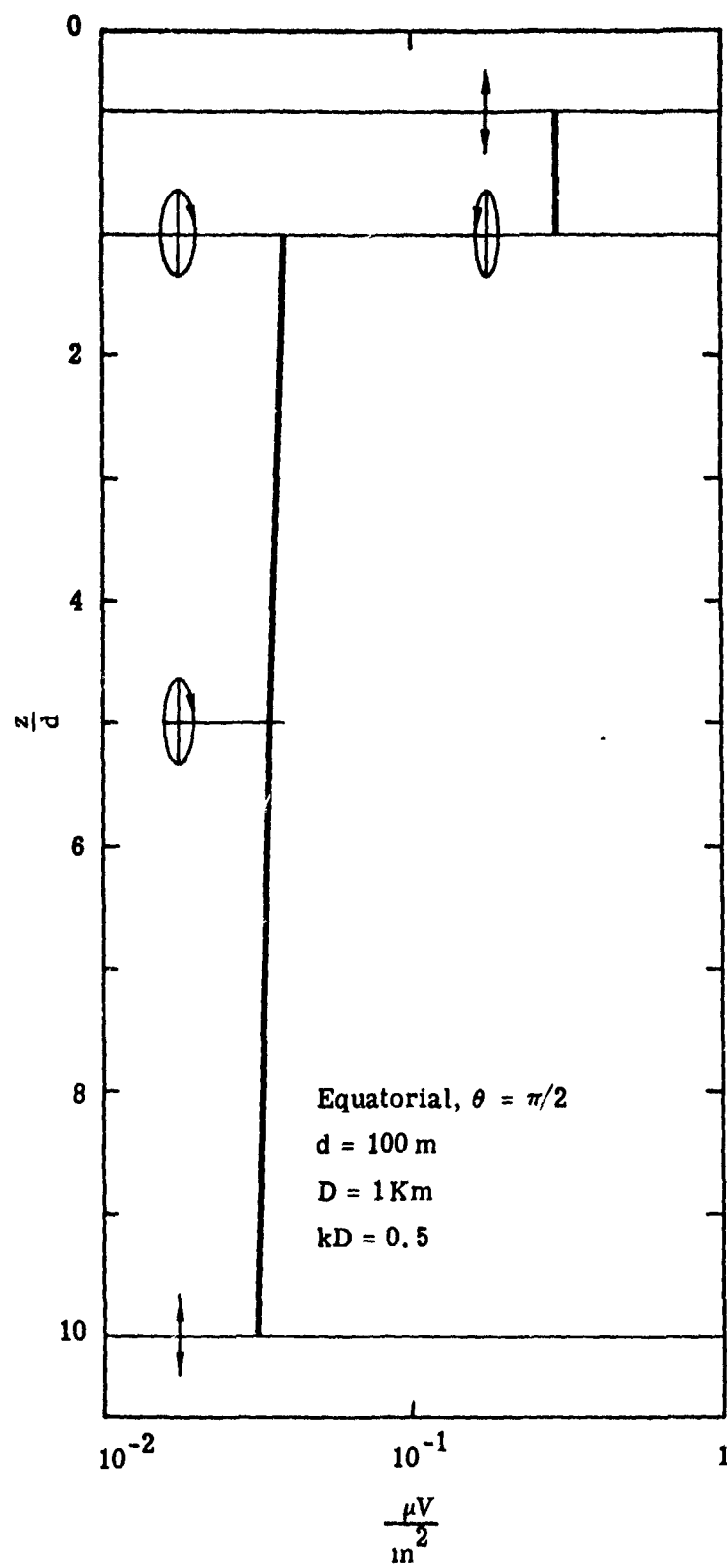


Figure 17b

REFERENCES

- Chapman, S., Solar plasma, geomagnetism, and aurora, in Geophysics, The Earth's Environment, Part III, p. 382, ed. C. DeWitt, et al., Gordon and Breach, Science Publishers, New York, 1962.
- Cox, C.S., J. H. Filloux, and J. C. Larsen, Electromagnetic studies of ocean currents and electrical conductivity below the ocean floor, Chapter 17 in The Sea, Vol. 4, Part I, A. E. Maxwell ed., John Wiley & Sons, New York, 1970.
- Crews, A., and J. Futterman, Geomagnetic micropulsations due to the motion of ocean waves, J. Geophys. Res., 67, 299-306, 1962.
- Faraday, M., Bakerian lecture: Experimental researches in electricity, Phil. Trans. Roy. Soc. London, part 1, 163, 1832.
- Groskaya, Ye. M., R. G. Skrymnikov, and G. V. Sokolov, Magnetic field variations induced by the motion of sea waves in shallow water, Geomagnetism and Aeronomy, (translation), 12, 131, 1972.
- Kozlov, A.N., G. A. Fonarev, and L.A. Shumov, Results of observations of the magnetic field of sea waves, Geomagnetism and Aeronomy, (translation), 11, 633, 1971.
- Kraichman, M.B., Handbook of electromagnetic propagation in conducting media, p. 2-3, NAVMAT P-2302, U.S. Government Printing Office, 1970.
- Kravtsov, A.G., and G.V. Sokolov, Variable magnetic field in the coastal zone, Geomagnetism and Aeronomy, (translation), 11, 783, 1971.

Lamb, H., Hydrodynamics, 6th ed., Cambridge University Press, London, pp.371-372, 1932.

Longuet-Higgins, M.S., M. E. Stern, and H. Stommel, The electrical field induced by ocean currents and waves, with applications to the method of towed electrodes, Papers in Physical Oceanography and Meteorology, 13(1), 1-37, 1954.

Longuet-Higgins, M.S., The statistical analysis of a random moving surface, Phil. Trans. Roy. Soc. London, A249, 321-387, 1957.

Maclure, K.C., R.A. Hafer, and J. T. Weaver, Magnetic variations produced by ocean swell, Nature, 204, 1290-1291, 1964.

Morse, P.M. and Feshbach, Methods of theoretical physics, Part II, Chapter 13, McGraw-Hill Book Company, New York, 1953.

Phillips, O.M., Dynamics of the upper ocean, p. 166, Cambridge Press, 1969.

Smythe, W.R., Static and dynamic electricity, Chapter X, McGraw-Hill Book Company, New York, 1968 (3rd Edition).

von Arx, W.S., An electromagnetic method for measuring the velocities of ocean currents from a ship under way, Pap. Phys. Ocean. Meteorol., 11(3), 1-62, 1950.

Warburton, F., and R. Caminiti, The induced magnetic field of sea waves, J. Geophys. Res., 69, 4311-4318, 1964.

Weaver, J.T., Magnetic variations associated with ocean waves and swell, J. Geophys. Res., 70, 1921-1929, 1965.

APPENDIX. PROFILES OF ELECTROMAGNETIC POTENTIALS

Profiles of electromagnetic fields induced by progressive waves in horizontally stratified oceans are specified by an electromagnetic potential profile, ϕ_s , and a velocity potential profile, ψ , as expressed by Equations (20a) and (20b) in Section II. The transverse-electric part of the field depends on both electromagnetic and velocity potential profiles, but the electrostatic part of the field depends on the velocity potential profile alone. In Sections III and IV, we described field profiles produced in deep and shallow seas, respectively, by progressive ocean waves having wavelengths much less than wavelengths of corresponding electromagnetic waves. First order expressions for field profiles are quite adequate provided wavelengths of surface waves are less than about 10 km and wavelengths of internal waves are less than about 100 km, and so are satisfactory for most purposes.

For completeness, however, we give here exact expressions for electromagnetic potential profiles generated by surface waves in an ocean of depth D and by internal waves in an ocean of depth D containing a sharp thermocline at a depth d . As in Section IV, we suppose that suboceanic conductivity profiles are adequately described by a poorly conducting layer, extending to a depth $D+h$, resting on a highly conducting layer extending indefinitely below the poorly conducting layer. But we do not further suppose, as in Section IV, that the poorly conducting layer is effectively a vacuum region of indefinite extent, although the supposition is adequate for ocean wavelengths less than a few tens of kilometers.

A. ELECTROMAGNETIC POTENTIAL PROFILE GENERATED BY SURFACE WAVES

The profile of the electromagnetic potential generated by a progressive surface wave in an ocean of depth D is given by

$$\phi_a = A_0 e^{kz} \quad (A1a)$$

above the surface ($z \leq 0$), by

$$\phi_s = C_1 e^{\alpha_1 z} + C_2 e^{-\alpha_2 z} \quad (A1b)$$

within the sea ($0 \leq z \leq D$), by

$$\phi_{c1} = 2C_3 \cosh \alpha_1 [z - (D + \hat{h})] \quad (A1c)$$

within the poorly conducting layer ($D \leq z \leq D + h$), and by

$$\phi_{c2} = 2C_3 \left(\frac{\alpha_1}{\alpha_2 + \alpha_1} \right) e^{\alpha_1 (\hat{h} - h)} e^{-\alpha_2 [z - (D + h)]} \quad (A1d)$$

within the highly conducting layer ($z \geq D + h$), where

$$e^{-2\alpha_1 (\hat{h} - h)} = \frac{\alpha_2 - \alpha_1}{\alpha_2 + \alpha_1} \quad (A1e)$$

defines the complex length \hat{h} and α_1 and α_2 correspond to conductivities of the poorly conducting and highly conducting layers, respectively.

The constants A_0 , C_1 , C_2 , and C_3 are expressed in terms of the value of the velocity potential profile at the surface, ψ_0 , by the relations

$$\begin{aligned}
A_0 = \frac{\psi_0 \sqrt{2}}{2 \gamma_+ \cosh kD} & \left\{ \left[\gamma_- e^{kD} - 2 \left(\frac{\alpha_1}{k} - \tanh \alpha_1 \tilde{h} \right) \right] (\vec{B} \cdot \hat{v}) \right. \\
& \left. + \left[\gamma_+ e^{-kD} - 2 \left(\frac{\alpha_1}{k} + \tanh \alpha_1 \tilde{h} \right) \right] (\vec{B} \cdot \hat{v}^*) \right\} \quad (A2a)
\end{aligned}$$

$$\begin{aligned}
C_1 = \frac{\psi_0 \sqrt{2}}{2 \gamma_+ \cosh kD} & \left\{ \left[2 \left(\frac{\alpha_1}{\alpha} - \tanh \alpha_1 \tilde{h} \right) e^{-(\alpha-k)D} \right. \right. \\
& - \left(1 + \frac{k}{\alpha} \right) \left(\frac{\alpha_1}{k} - \tanh \alpha_1 \tilde{h} \right) \right] (\vec{B} \cdot \hat{v}) \\
& - \left(1 + \frac{k}{\alpha} \right) \left(\frac{\alpha_1}{k} + \tanh \alpha_1 \tilde{h} \right) (\vec{B} \cdot \hat{v}^*) \left. \right\} \quad (A2b)
\end{aligned}$$

$$\begin{aligned}
C_2 = \frac{-\psi_0 \sqrt{2}}{2 \gamma_+ \cosh kD} & \left\{ \left[2 \left(\frac{\alpha_1}{\alpha} + \tanh \alpha_1 \tilde{h} \right) e^{(\alpha+k)D} \right. \right. \\
& + \left(1 - \frac{k}{\alpha} \right) \left(\frac{\alpha_1}{k} - \tanh \alpha_1 \tilde{h} \right) \right] (\vec{B} \cdot \hat{v}) \\
& + \left(1 - \frac{k}{\alpha} \right) \left(\frac{\alpha_1}{k} + \tanh \alpha_1 \tilde{h} \right) (\vec{B} \cdot \hat{v}^*) \left. \right\} \quad (A2c)
\end{aligned}$$

and

$$2C_3 \sinh \alpha_1 \tilde{h} = C_1 e^{\alpha D} + C_2 e^{-\alpha D} + \frac{\psi_0 (\vec{B} \cdot \hat{z})}{\cosh kD} \quad (A2d)$$

where

$$\gamma_{\pm} = 2 \cosh \alpha D \left[\frac{\alpha_1}{k} \pm \frac{\alpha_1}{a} \tanh \alpha D + \left(\frac{\alpha}{k} \tanh \alpha D \pm 1 \right) \tanh \alpha_1 \tilde{h} \right] . \quad (\text{A2e})$$

Wave height of surface waves is related to the value of the velocity potential profile at the surface by the expression

$$i \left(\frac{\omega}{k} \right) \xi_0 = \psi_0 \tanh kD . \quad (\text{A2i})$$

As kD becomes large, we note that the constants C_1 and C_3 vanish,

$$A_0 \equiv \left(\frac{\alpha - k}{\alpha + k} \right) \psi_0 \sqrt{2} (B \cdot \hat{v}) , \quad (\text{A3a})$$

and

$$C_2 \equiv - \left(\frac{2k}{\alpha + k} \right) \psi_0 \sqrt{2} (B \cdot \hat{v}) . \quad (\text{A3b})$$

B. ELECTROMAGNETIC POTENTIAL PROFILE GENERATED BY INTERNAL WAVES

The profile of the electromagnetic potential generated by a progressive internal wave in an ocean of depth D containing a sharp thermocline at a depth d is given by

$$\phi_a = A_0 e^{kz} \quad (\text{A4a})$$

above the surface ($z \leq 0$), by

$$\phi_{s1} = C_{11} e^{\alpha z} + C_{12} e^{-\alpha z} \quad (\text{A4b})$$

above the thermocline ($d \leq z \leq D$), by

$$\phi_{s2} = C_{21} e^{\alpha(z-d)} + C_{22} e^{-\alpha(z-d)} \quad (\text{A4c})$$

below the thermocline ($d \leq z \leq D$), by

$$\phi_{c1} = 2C_3 \cosh \alpha_1 [z - (D+\tilde{h})] \quad (\text{A4d})$$

within the poorly conducting layer ($d \leq z \leq D+h$), and by

$$\phi_{c2} = 2C_3 \left(\frac{\alpha_1}{\alpha_2 + \alpha_1} \right) e^{\alpha_1(\tilde{h}-h)} e^{-\alpha_2[z-(D+h)]} \quad (\text{A4e})$$

within the highly conducting layer ($z \geq D+h$), where the complex length \tilde{h} is defined as before [Equation (A1e)].

The constants A_0 , C_{11} , C_{12} , C_{21} , C_{22} , and C_3 are expressed in terms of the value of the velocity potential profile at the surface, ψ_0 , by the relations

$$\begin{aligned} A_0 = & \frac{\psi_0 \sqrt{2}}{2 \gamma_+ \sinh k(D-d)} \left\{ \left[\gamma_- \sinh k(D-d) - G_- \sinh kD \right. \right. \\ & + 2 \sinh kd \left(\frac{\alpha_1}{k} - \tanh \alpha_1 \tilde{h} \right) \left. \right] (\vec{B} \cdot \hat{v}) \\ & + \left[\gamma_+ \sinh k(D-d) - G_+ \sinh kD \right. \\ & \left. \left. + 2 \sinh kd \left(\frac{\alpha_1}{k} + \tanh \alpha_1 \tilde{h} \right) \right] (\vec{B} \cdot \hat{v}^*) \right\} \quad (\text{A5a}) \end{aligned}$$

$$\begin{aligned}
4 \frac{\alpha}{k} C_{11} &= -\psi_0 \sqrt{2} \left[\left(\frac{\alpha}{k} - 1 \right) (\vec{B} \cdot \hat{v}) + \left(\frac{\alpha}{k} + 1 \right) (\vec{B} \cdot \hat{v}^*) \right] \\
&+ 2A_0 \left(\frac{\alpha}{k} + 1 \right)
\end{aligned} \tag{A5b}$$

$$\begin{aligned}
4 \frac{\alpha}{k} C_{12} &= -\psi_0 \sqrt{2} \left[\left(\frac{\alpha}{k} + 1 \right) (\vec{B} \cdot \hat{v}) + \left(\frac{\alpha}{k} - 1 \right) (\vec{B} \cdot \hat{v}^*) \right] \\
&+ 2A_0 \left(\frac{\alpha}{k} - 1 \right)
\end{aligned} \tag{A5c}$$

$$\begin{aligned}
4 \frac{\alpha}{k} C_{21} &= \frac{\psi_0 \sinh kD}{\sinh k(D-d)} \left[\left(\frac{\alpha}{k} - 1 \right) (\vec{B} \cdot \hat{v}) + \left(\frac{\alpha}{k} + 1 \right) (\vec{B} \cdot \hat{v}^*) \right] \sqrt{2} \\
&+ 4 \frac{\alpha}{k} C_{11} e^{\alpha d}
\end{aligned} \tag{A5d}$$

$$\begin{aligned}
4 \frac{\alpha}{k} C_{22} &= \frac{\psi_0 \sinh kD}{\sinh k(D-d)} \left[\left(\frac{\alpha}{k} + 1 \right) (\vec{B} \cdot \hat{v}) + \left(\frac{\alpha}{k} - 1 \right) (\vec{B} \cdot \hat{v}^*) \right] \sqrt{2} \\
&+ 4 \frac{\alpha}{k} C_{12} e^{-\alpha d}
\end{aligned} \tag{A5e}$$

and

$$2C_3 \sinh \alpha_1 \hat{h} = \frac{-\psi_0 \sinh kd}{\sinh k(D-d)} (\vec{B} \cdot \hat{z}) + C_{22} e^{-\alpha(D-d)} + C_{21} e^{\alpha(D-d)} \quad (A5f)$$

where

$$G_{\pm} = 2 \cosh \alpha(D-d) \left[\frac{\alpha_1}{k} \pm \frac{\alpha_1}{\alpha} \tanh \alpha(D-d) + \left(\frac{\alpha}{k} \tanh \alpha(D-d) \pm 1 \right) \tanh \alpha_1 \hat{h} \right] \quad (A5g)$$

and γ_{\pm} is defined by Equation (A2e).

The thermocline displacement, or wave height of an internal wave, ζ_d , is related to the value of the velocity potential profile at the surface by the expression

$$i \left(\frac{\omega}{k} \right) \zeta_d = -\psi_0 \sinh kd \quad (A6)$$

As kD becomes large, the constants C_{21} and C_3 vanish,

$$A_0 \approx \frac{\psi_0}{\sqrt{2}} \left(1 - e^{-(\alpha-k)d} \right) \left[\left(\frac{\alpha-k}{\alpha+k} \right) (\vec{B} \cdot \hat{v}) + (\vec{B} \cdot \hat{v}^*) \right], \quad (A7a)$$

$$C_{11} \approx \frac{-\psi_0}{2\sqrt{2}} \left(1 + \frac{k}{\alpha} \right) e^{-(\alpha-k)d} \left[\left(\frac{\alpha-k}{\alpha+k} \right) (\vec{B} \cdot \hat{v}) + (\vec{B} \cdot \hat{v}^*) \right], \quad (A7b)$$

$$C_{12} \cong \frac{-\psi_0}{2\sqrt{2}} \left(1 + \frac{k}{\alpha}\right) \left\{ \left[1 - \left(\frac{\alpha - k}{\alpha + k}\right)^2 \left(1 - e^{-(\alpha - k)d}\right) \right] (\vec{B} \cdot \hat{v}) \right. \\ \left. + \left(\frac{\alpha - k}{\alpha + k}\right) e^{-(\alpha - k)d} (\vec{B} \cdot \hat{v}^*) \right\} \quad (A7c)$$

and

$$C_{22} \cong \frac{\psi_0}{2\sqrt{2}} \left(1 + \frac{k}{\alpha}\right) e^{-\alpha d} \left\{ \left[e^{(\alpha + k)d} - 1 + \left(\frac{\alpha - k}{\alpha + k}\right)^2 \left(1 - e^{-(\alpha - k)d}\right) \right] (\vec{B} \cdot \hat{v}) \right. \\ \left. + \left(\frac{\alpha - k}{\alpha + k}\right) \left(e^{(\alpha + k)d} - e^{-(\alpha - k)d} \right) (\vec{B} \cdot \hat{v}^*) \right\} . \quad (A7d)$$

Furthermore, as kd becomes large, which implies that kD is also large, the constants C_{21} , C_3 , and C_{11} vanish,

$$A_0 \cong \frac{\psi_0}{\sqrt{2}} \left[\left(\frac{\alpha - k}{\alpha + k}\right) (\vec{B} \cdot \hat{v}) + (\vec{B} \cdot \hat{v}^*) \right] , \quad (A8a)$$

$$C_{12} \cong -\psi_0 \sqrt{2} \left(\frac{k}{\alpha + k}\right) (\vec{B} \cdot \hat{v}) \quad (A8b)$$

and

$$C_{22} \cong \frac{\psi_0 e^{kd}}{2\sqrt{2}} \left(1 + \frac{k}{\alpha}\right) \left[(\vec{B} \cdot \hat{v}) + \left(\frac{\alpha - k}{\alpha + k}\right) (\vec{B} \cdot \hat{v}^*) \right] . \quad (A8c)$$